HHS Public Access

Author manuscript

Cell Rep. Author manuscript; available in PMC 2023 October 23.

Published in final edited form as:

Cell Rep. 2023 February 28; 42(2): 112073. doi:10.1016/j.celrep.2023.112073.

Crosstalk between ILC2s and Th2 cells varies among mouse models

Rama K. Gurram[1,2,*], **Danping Wei**[1], **Qiao Yu**[1,3], **Matthew J. Butcher**[1], **Xi Chen**[1], **Kairong Cui**[4], **Gangqing Hu**[4,5], **Mingzhu Zheng**[1], **Xiaoliang Zhu**[1], **Jangsuk Oh**[2], **Bing Sun**[6], **Joseph F. Urban Jr.**[7], **Keji Zhao**[4], **Warren J. Leonard**[2], **Jinfang Zhu**[1,8,*]

[1]Molecular and Cellular Immunoregulation Section, Laboratory of Immune System Biology, National Institute of Allergy and Infectious Diseases, National Institutes of Health, Bethesda, MD 20892, USA

[2]Laboratory of Molecular Immunology and the Immunology Center, National Heart, Lung, and Blood Institute, Bethesda, MD 20892, USA

[3]Department of Gerontology and Respirology, Xiangya Hospital, Central South University, Changsha, Hunan 410008, China

[4]Laboratory of Epigenome Biology, National Heart, Lung, and Blood Institute, National Institutes of Health, Bethesda, MD 20892, USA

[5]Department of Microbiology, Immunology, and Cell Biology, School of Medicine, West Virginia University, Morgantown, WV 26506, USA

[6]State Key Laboratory of Cell Biology, CAS Center for Excellence in Molecular Cell Science, Shanghai Institute of Biochemistry and Cell Biology, Chinese Academy of Sciences, University of Chinese Academy of Sciences, Shanghai 200031, China

[7]US Department of Agriculture, Agricultural Research Service, Beltsville Agricultural Research Center, Animal Parasitic Diseases Laboratory, Beltsville, MD 20705, USA

[8]Lead contact

SUMMARY

Type 2 T helper (Th2) cells and group 2 innate lymphoid cells (ILC2s) provide protection against helminth infection and are involved in allergic responses. However, their relative importance and crosstalk during type 2 immune responses are still controversial. By generating and utilizing

*Correspondence: rama.gurram@nih.gov (R.K.G.), jfzhu@niaid.nih.gov (J.Z.).

AUTHOR CONTRIBUTIONS

R.K.G. and J.Z. conceived the project; R.K.G. performed most of the experiments; D.W., Q.Y., M.J.B., X.Z., and M.Z. performed some experiments; K.C. and X.C. contributed to the RNA-seq experiments; G.H. and R.K.G. performed bioinformatic analysis; J.O. maintained the *Crlf2*$^{-/-}$ mice for related experiments; J.F.U. provided critical reagents and technical suggestions; W.J.L., K.Z., B.S., and J.F.U. made intellectual contributions and edited the manuscript; R.K.G. and J.Z. wrote the manuscript; J.Z. supervised the project.

SUPPLEMENTAL INFORMATION

Supplemental information can be found online at https://doi.org/10.1016/j.celrep.2023.112073.

DECLARATION OF INTERESTS

The authors declare no competing interests.

mouse strains that are deficient in either ILC2s or Th2 cells, we report that interleukin (IL)-33-mediated ILC2 activation promotes the Th2 cell response to papain; however, the Th2 cell response to ovalbumin (OVA)/alum immunization is thymic stromal lymphopoietin (TSLP) dependent but independent of ILC2s. During helminth infection, ILC2s and Th2 cells collaborate at different phases of the immune responses. Th2 cells, mainly through IL-4 production, induce the expression of IL-25, IL-33, and TSLP, among which IL-25 and IL-33 redundantly promote ILC2 expansion. Thus, while Th2 cell differentiation can occur independently of ILC2s, activation of ILC2s may promote Th2 responses, and Th2 cells can expand ILC2s by inducing type 2 alarmins.

Graphical abstract

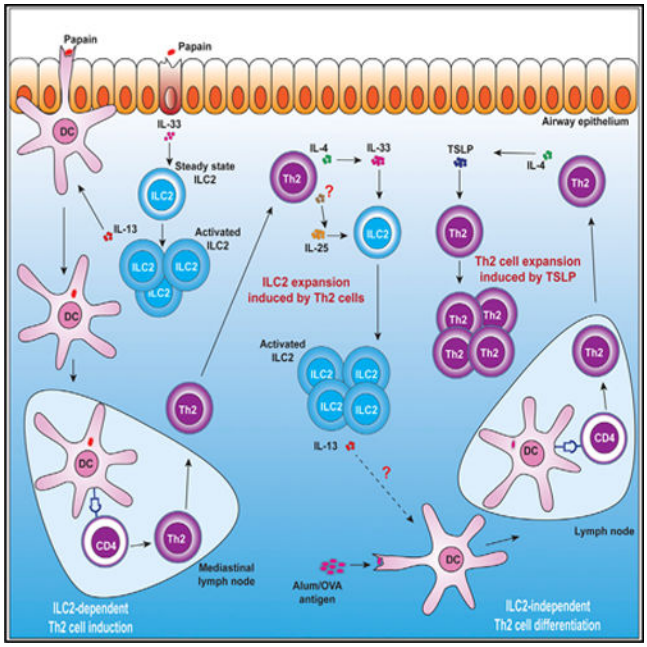

In brief

ILC2s and Th2 cells are involved in a variety of type 2 immune responses. Gurram et al. report that the crosstalk between ILC2s and Th2 cells varies among mouse models and is mediated by type 2 alarmins and IL-4.

INTRODUCTION

Type 2 immune responses provide protection against helminth infection and induce allergic inflammatory diseases; both processes can be driven by type 2 T helper (Th2) cells and group 2 innate lymphoid cells (ILC2s), with ILC2s serving as an innate counterpart of adaptive effector Th2 cells.[1–4] Th2 cell differentiation requires T cell receptor (TCR)-mediated signaling triggered by the major histocompatibility complex (MHC) class II-peptide complex on dendritic cells (DCs)[5]; however, ILC2s are preexisting tissue-resident type 2 lymphocytes.[6–8] While inducing adaptive immune responses, allergen exposure or helminth infection may first upregulate the release of alarmins such as interleukin (IL)-33

by non-hematopoietic cells to activate and expand ILC2s.[9] The commitment of effector Th2 cell differentiation is controlled by the master transcription factor GATA-binding protein 3 (GATA3).[10–14] Fate determination and maintenance of ILC2s are also under the control of GATA3.[15–17]

Although ILC2s and Th2 cells exhibit similar effector functions, their relative contributions and interdependency have been controversial. ILC2s were previously reported to induce Th2 cell response directly by cell-cell interactions[18–20] and indirectly by secreting IL-13 to induce DC migration to the draining lymph node.[21,22] ILC2s were also shown to be dispensable for Th2 cell differentiation during helminth infection.[23] Th2 cells may induce ILC2 expansion through the production of IL-2[18,24] or IL-4.[25] However, the potential roles of ILC2-activating alarmins during this process remain unclear. Finally, the relative importance of Th2 cells and ILC2s during type 2 immune responses is still elusive.

Some controversies regarding the relative importance of and crosstalk between ILC2s and Th2 cells could be partly due to the use of different animal models and procedures. Most importantly, specific ILC2- or Th2-deficient mouse strains without affecting the other compartment are still lacking. Here, we report mouse strains that are deficient in either ILC2s or Th2 cells with a high degree of specificity. By using these mice, we investigated the crosstalk between ILC2s and Th2 cells in various models involving type 2 immune responses. Our results demonstrate that the division of labor and crosstalk between ILC2s and Th2 cells in orchestrating type 2 immune responses are model and stage dependent and that type 2 alarmins play critical roles during both the initiation and expansion phases of type 2 immune responses.

RESULTS

Klrg1^{Cre}-mediated *Gata3* deletion specifically depletes ILC2s

Killer cell lectin like receptor G1 (KLRG1), a c-type lectin inhibitory receptor expressed on CD8$^+$ T cells and natural killer (NK) cells,[26,27] is also highly expressed by most ILC2s.[15,28] In the type 2 pulmonary inflammation mouse model chronically challenged with the protease papain (Figure 1A), KLRG1 was also found to be expressed by the majority of ILC2s, whereas only a small subset of Th2 cells expressed KLRG1 (Figure S1A). Other immune cells involved in type 2 immune responses did not express KLRG1. Because KLRG1 was preferentially expressed by ILC2s (Figure 1B) and GATA3 is required for the maintenance of ILC2s,[15–17] *Klrg1*^{Cre}-mediated *Gata3* deletion could eliminate ILC2s without affecting Th2 cells. Indeed, ILC2s in the lung of naive *Klrg1*^{Cre}*Gata3*$^{fl/fl}$ mice were depleted, while other lymphoid subsets, including ILC1s, ILC3s, NK cells, and CD4$^+$ T (both Foxp3$^+$ and Foxp3$^-$ populations) cells, were intact (Figures 1C and S1B). ILC2s, but not ILC3s, in the small intestine lamina propria (siLP) of naive *Klrg1*^{Cre}*Gata3*$^{fl/fl}$ mice were also undetectable (Figure S1C). In wild-type (WT) mice chronically challenged with papain, known to induce type 2 lung inflammation,[29] less than 5% of Th2 cells and CD8$^+$ T cells expressed KLRG1, whereas ~40% of NK cells expressed KLRG1 (Figures S1D and S1E). Fate-mapping experiments showed that less than 5% of Th2 cells, ~12% of NK cells, and virtually no CD8$^+$ T cells expressed the fate mapping marker tdTomato in the *Klrg1*^{Cre}*Gata3*$^{fl/fl}$*R26*^{tdTomato} mice (Figures S1F and S1G). Thus, *Klrg1*^{Cre}-mediated *Gata3*

gene deletion had a minimal effect on Th2 cells, $CD8^+$ T cells, and NK cells at least in the papain system examined.

ILC2s promote the generation of Th2 cells induced by papain

Short-term (acute) papain challenges of mice activate lung ILC2s without inducing effector Th2 cells, whereas prolonged (chronic) papain challenges also induce Th2 cell differentiation. Therefore, we performed experiments with mice intranasally challenged with papain on days 0, 1, and 2 (acute phase), followed by papain re-challenge on days 13, 14, and 15 (chronic phase) (Figure 1A). The gating strategy for identifying and analyzing ILC2s, Th2 cells, and eosinophils is shown in Figures S2A and S2B. Although both acute and chronic challenges induced eosinophilia, chronic papain challenges induced markedly increased eosinophils in the lung and bronchoalveolar fluid (BAL) fluid (Figures S3A and S3B). As expected, acute papain challenges induced ILC2 activation but not Th2 response (Figures S3C and S3D). By contrast, chronic papain challenges not only induced Th2 cells but also further expanded ILC2s (Figures S3C and S3D).

In the ILC2-deficient ($Klrg1^{Cre}Gata3^{fl/fl}$) mice, diminished numbers of eosinophils in BALF and lungs were noted during acute papain challenges (Figure 1D). However, the $Klrg1^{Cre}Gata3^{fl/fl}$ mice chronically challenged with papain only exhibited reduced eosinophilia (Figure 1E) compared with the $Gata3^{fl/fl}$ mice. The $Klrg1^{Cre}Gata3^{fl/fl}$ mice also exhibited lower numbers of Th2 cells (Figure 1F). In addition, the $Klrg1^{Cre}Gata3^{fl/fl}$ displayed reduced inflammation with significantly fewer eosinophils and a reduced trend of overall lung histopathology (Figures 1G and 1H).

We then used the OVA-induced Th2 model (Figure 1I). In this model, both $Gata3^{fl/fl}$ and $Klrg1^{Cre}Gata3^{fl/fl}$ mice exhibited equal severity of eosinophilia and same numbers of Th2 cells (Figure 1J). Some activated regulatory T cells (Tregs) may express high levels of KLRG1,[30] and thus $Klrg1^{Cre}$-mediated *Gata3* gene deletion in this Treg population could indirectly affect Th2 cell responses. However, the $Foxp3^{Cre}Gata3^{fl/fl}$ mice displayed more severe eosinophilia and generated more Th2 cells (Figures S3E–S3H), consistent with the current notion that *Gata3*-deficient Tregs are defective in limiting Th2 responses.[31,32] Finally, transfer of ILC2s into the $Klrg1^{Cre}Gata3^{fl/fl}$ mice followed by chronic papain challenges partially rescued the Th2 response in ILC2-deficient mice (Figure 1K).

To further investigate the role of ILC2s in antigen-specific Th2 response, we used papain as an adjuvant in immunizing mice with the 2W1S peptide (Figure 1L), an $I\text{-}A^b$-binding peptide variant derived from the murine $I\text{-}E^d$ MHC class II α chain, which is highly immunogenic in C57BL/6 mice.[33] 2W1S:I-Ab tetramer-positive $CD4^+$ T cells were induced in the 2W1S-immunized $Gata3^{fl/fl}$ mice that also received papain as an adjuvant but not in mice that received 2W1S alone (Figures 1M and 1N). The adjuvant effect of papain requires ILC2s since the ILC2-deficient $Klrg1^{Cre}Gata3^{fl/fl}$ mice failed to generate 2W1S-specific $CD4^+$ T cells in response to 2W1S-papain immunization. Antigen-induced airway inflammation with alum as the adjuvant shown in Figure 1I was also tested with the 2W1S peptide. In the alum model, both $Gata3^{fl/fl}$ and $Klrg1^{Cre}Gata3^{fl/fl}$ mice generated similar numbers of 2W1S:$I\text{-}A^b$ tetramer-specific $CD4^+$ T cells (Figures 1M and 1N), and these antigen-specific cells expressed high levels of GATA3 (Figure 1O).

IL-33 plays an essential role in the initiation of ILC2-mediated Th2 cell generation

Since type 2 alarmins (IL-33, IL-25, and TSLP) play an important role in the activation of ILC2s, we first measured the production of these alarmins in both papain and ovalbumin (OVA)/alum-induced airway inflammation models. While papain primarily induced the expression of IL-33 during the acute phase, it induced the production of all three alarmins during the chronic phase (Figure 2A). On the other hand, in the OVA/alum model, TSLP was first induced 2 days after OVA challenges (Figure 2B); after 4 consecutive days of OVA challenges, all three alarmins were induced.

We then performed acute and chronic papain challenges with mice deficient in CIKS, an adaptor molecule required for IL-25-mediated signaling,[34] IL-33-deficient (IL-33 trap) mice,[35] or *Crlf2*$^{-/-}$ (a TSLP receptor subunit knockout) mice.[36] Interestingly, mice deficient in either CIKS or *Crlf2*$^{-/-}$ had similar severity of eosinophilia as WT mice during acute papain challenge. By contrast, IL-33-deficient mice had far fewer eosinophils in the BALF and lungs (Figure 2C). Furthermore, the ILC2s from IL-33-deficient mice were poor IL-13 producers (Figure 2D).

In the chronic papain challenge model, CIKS knockout (KO) mice and *Crlf2*$^{-/-}$ mice also showed similar levels of eosinophilia in BALF and lungs as WT mice (Figure 2E), but IL-33-deficient mice had fewer eosinophils. Accordingly, while the Th2 cell response was greatly reduced in IL-33-deficient mice, normal numbers of Th2 cells were detected in the absence of IL-25 or TSLP signaling (Figure 2F). Furthermore, IL-33 trap mice had far fewer ILC2s in response to chronic papain challenges compared with mice in other groups (Figure 2G), and the histopathological analysis of lung tissues revealed that IL-33-deficient mice had lower histopathological scores and fewer eosinophils in the tissue compared with their WT counterparts in both acute and chronic papain challenge models (Figures 2H and 2I). Therefore, IL-33, but not IL-25 or TSLP, is required for the activation of ILC2s in response to acute papain challenge and for ILC2-mediated promotion of Th2 cell lung accumulation during chronic papain challenge.

The inability of IL-33-deficient mice to mount a strong Th2 response to chronic papain challenges was further demonstrated by the lack of activated CD40^{+} DC migration into the mediastinal lymph node during acute papain challenges (Figures S4A and S4B). Furthermore, the ILC2-deficient *Klrg1*^{Cre}*Gata3*$^{fl/fl}$ mice acutely challenged with papain also had significantly fewer numbers of CD40^{+} DCs in the mediastinal lymph node than the *Gata3*$^{fl/fl}$ mice (Figures S4C and S4D). These results are consistent with an earlier report that IL-13 produced by ILC2s promotes the migration of activated DCs to the draining lymph nodes.[21]

TSLP is the major alarmin for ILC2-independent Th2 cell induction by OVA/alum immunization

In contrast to the results with the papain model, in the OVA-alum immunization model in which ILC2-independent Th2 cell differentiation was observed, IL-33 trap mice showed significantly higher eosinophilia (Figures 3A and 3B) with increased numbers of effector Th2 cells (Figure 3C). The enhanced Th2 response in IL-33-deficient mice may have

resulted from the requirement of IL-33 signaling in Tregs to suppress effector T cell responses.[37,38] The CIKS KO mice also had more eosinophils and Th2 cells in the OVA/alum model (Figures 3D–3F). By contrast, OVA/alum-induced type 2 immune response in the *Crlf2*$^{-/-}$ mice was significantly reduced compared with the WT mice (Figures 3G–3I). Furthermore, preconditioning the mice with TSLP (200 ng) intranasally (Figure 3J) significantly enhanced Th2 responses during OVA intranasal (i.n.) challenges in both WT (Figure 3K) and ILC2-deficient mice (Figure 3L). These results indicate that TSLP is a major promoter of ILC2-independent Th2 cell response in the OVA/alum model.

ILC2 pre-activation promotes the Th2 cell response in the OVA/alum model

To gain more insights into the differential dependence of ILC2s between the papain- and OVA/alum-induced airway inflammation, we tested whether ILC2 activation induced by cytokine stimulation could promote the ILC2-independent Th2 cell response in the OVA/alum model. Therefore, we first used IL-33 i.n. challenges on days 8 and 9 during the OVA/alum-induced airway inflammation model (Figure S4E). WT *Gata3*$^{fl/fl}$ mice that received IL-33 had significantly higher eosinophilia and higher Th2 cell numbers compared with the mice that did not receive IL-33 (Figure S4F). However, the Th2 cell response in the ILC2-deficient *Klrg1*^{Cre}*Gata3*$^{fl/fl}$ mice was not enhanced by IL-33 administration (Figure S4G). Pre-treating *Gata3*$^{fl/fl}$ mice with IL-25 intraperitoneally (i.p.) for 3 days (Figure S4H) also induced more eosinophils and Th2 cells compared with without pre-treatment (Figure S4I). However, the ILC2-deficient *Klrg1*^{Cre}*Gata3*$^{fl/fl}$ mice failed to show such a response to IL-25 (Figure S4J). Therefore, even in a Th2 model where ILC2s are not required, ILC2 activation may further promote the Th2 response.

The adaptive lymphocyte compartment is necessary for a robust expansion of ILC2s

Dramatically increased total ILC2 number during the chronic stage of papain challenges (Figure S3C) was correlated with enhanced production of IL-25, TSLP, and IL-33 (i.e., all three type 2 alarmins; Figure 2A). Since Th2 cells were induced during this chronic stage (Figure S3D), we further investigated the role of effector Th2 cells in ILC2 expansion. We first performed the acute and chronic papain challenges using *Rag1*$^{-/-}$ mice. *Rag1*$^{-/-}$ mice acutely challenged with papain (i.n.) showed an increase in eosinophilia in BALF and lungs (Figures 4A and 4B). Possibly because of the lymphopenic environment in the *Rag1*$^{-/-}$ mice, they had more ILC2s than WT mice at steady state and upon acute papain challenges (Figure 4C). By contrast, WT mice chronically challenged with papain exhibited much greater eosinophilia than did similarly treated *Rag1*$^{-/-}$ mice (Figures 4A and 4B). Although additional Th2 cells in the WT mice may contribute to the eosinophilia, WT mice also had more ILC2s after chronic papain challenge compared with the *Rag1*$^{-/-}$ mice (Figure 4C). Nevertheless, a similar percentage of IL-5- and IL-13-expressing ILC2s was observed in the WT and *Rag1*$^{-/-}$ animals, suggesting that these ILC2s might be functionally similar (Figure 4D). These results indicate that adaptive immune cells may positively regulate the expansion of ILC2s.

Th2 cells are necessary and sufficient in inducing ILC2 expansion

To test whether Th2 cells in the adaptive lymphocyte compartment are responsible for ILC2 expansion, we generated h*CD2*^{Cre} *Gata3*$^{fl/fl}$ (Th2-deficient) mice. Naive CD4^{+} T

cells from the h*CD2*^{Cre}*Gata3*$^{fl/fl}$ mice showed a similar ability, compared with WT naive cells, to differentiate into effector Th1 and Th17 cells *in vitro*, judged by interferon γ (IFNγ) and IL-17 expression, respectively (Figures S5A and S5B). As expected, h*CD2*^{Cre} *Gata3*$^{fl/fl}$ cells were markedly defective in differentiating into IL-13-producing Th2 cells (Figure S5C). Furthermore, *Rag1*$^{-/-}$ mice that received naive CD4^{+} T cells from either WT (*Gata3*$^{fl/fl}$) or Th2-deficient mice (h*CD2*^{Cre}*Gata3*$^{fl/fl}$) developed equivalent colitis as judged by their weight loss (Figure S5D), and CD4^{+} T cells from both groups express similar levels of IFNγ (Figures S5E and S5F). We then challenged these Th2-deficient mice with papain. Although both *Gata3*$^{fl/fl}$ and h*CD2*^{Cre}*Gata3*$^{fl/fl}$ mice had similar numbers of eosinophils (Figures 4E and 4F) and ILC2s during acute papain challenges (Figure 4G), the h*CD2*^{Cre}*Gata3*$^{fl/fl}$ mice chronically challenged with papain showed a milder type 2 immune pathology with significantly fewer eosinophils compared with similarly treated *Gata3*$^{fl/fl}$ mice. Notably, the h*CD2*^{Cre}*Gata3*$^{fl/fl}$ mice had much fewer ILC2s compared with the *Gata3*$^{fl/fl}$ mice after chronic papain challenge. However, ILC2s from both groups were equally capable of expressing type 2 cytokines (Figure 4H). Furthermore, histopathological analyses of lung tissues revealed that although the h*CD2*^{Cre}*Gata3*$^{fl/fl}$ mice exhibited similar severity of eosinophilia and inflammation compared with the *Gata3*$^{fl/fl}$ mice during acute papain challenge, the h*CD2*^{Cre}*Gata3*$^{fl/fl}$ mice were unable to mount a severe inflammation during the chronic stage of papain challenges (Figures 4I and 4J).

As shown above, mice sensitized with OVA-alum i.p. followed by OVA i.n. challenges could elicit an ILC2-independent Th2 response (Figures 1J and 1K). However, during this process, ILC2s also expanded (Figures 4K and 4L). To provide direct evidence to support the notion that Th2 cells can induce ILC2 expansion, we adoptively transferred *in-vitro*-differentiated OT-II-Th2 cells and then i.n. challenged these mice with OVA (Figure 4M). Mice receiving *in-vitro*-differentiated OT-II Th2 cells elicited a type 2 immune response upon i.n. OVA challenges (Figure 4N). Even in this transfer model, endogenous ILC2s were expanded and activated with an increased capacity in IL-5 and IL-13 production (Figure 4N), suggesting that Th2 cells are capable of inducing the expansion and activation of ILC2s.

Adaptive lymphocytes do not affect the transcriptome of ILC2s

To further understand the impact of adaptive lymphocytes on ILC2s at the genome-wide level, we performed RNA sequencing (RNA-seq) analyses on ILC2s from WT and *Rag1*$^{-/-}$ animals chronically challenged with papain. Based on the principal-component analysis (PCA), the ILC2s from WT and *Rag1*$^{-/-}$ mice had a similar transcriptomic profile (Figure 5A), with very few genes significantly differing in their expression in ILC2s from WT versus *Rag1*$^{-/-}$ animals (Figure 5B). In addition, the type 2-related genes were similarly upregulated by papain challenges in both WT and *Rag1*$^{-/-}$ ILC2s (Figure 5C).

Th2 cells induce the expression of type 2 alarmins

ILC2s proliferate and produce IL-5 and IL-13 in response to IL-25, IL-33, or TSLP stimulation.[39,40] To assess whether Th2 cells are required for inducing the expression of type 2 alarmins, we performed papain challenges using the Th2-deficient mice (h*CD2*^{Cre}*Gata3*$^{fl/fl}$). As expected, similar levels of IL-33 release were detected in h*CD2*^{Cre}*Gata3*$^{fl/fl}$ and their WT counterpart *Gata3*$^{fl/fl}$ mice acutely challenged with papain

(Figure 5D). By contrast, h*CD2*^{Cre}*Gata3*$^{fl/fl}$ mice chronically challenged with papain showed diminished levels of all three type 2 alarmins in the BALF compared with the *Gata3*$^{fl/fl}$ mice.

Interestingly, OVA-induced pulmonary inflammation caused by Th2 cells generated in the periphery also upregulated the type 2 alarmin levels in the BALF (Figure 2B). To exclude the possibility that adjuvant was responsible for the induction of type 2 alarmins, we injected *in-vitro*-differentiated OT-II-Th2 cells into recipient mice and i.n. challenged them with OVA antigen. The levels of all three type 2 alarmins were significantly increased by the adoptive transfer of antigen-specific Th2 cells (Figure 5E), confirming an important function of Th2 cells for their induction.

IL-25 and IL-33 redundantly mediate ILC2 expansion induced by Th2 cells

To test whether Th2 cells activate and expand ILC2s by inducing the release of type 2 alarmins, we used a Th2 cell transfer model to assess the expansion of ILC2s in the mice deficient in either individual type 2 alarmin or its receptor. Notably, ILC2s in mice deficient for either CIKS, IL-33, or TSLPR expanded similarly to ILC2s in WT mice (Figure 5F), indicating that no individual alarmin is absolutely required for this function. By injecting the WT and IL-33-deficient mice with various combinations of neutralizing anti-IL-25 and anti-TSLP antibodies to block these signaling pathways separately or together, we found that ILC2 expansion driven by Th2 cells was significantly reduced when both IL-33 and IL-25 signaling pathways were blocked (Figure 5G). Blockade of TSLP signaling did not result in a further reduction. Indeed, treatment with either IL-25 or IL-33, but not TSLP, was able to activate pulmonary ILC2s isolated from naive mice *in vitro* (Figure 5H). Collectively, our results demonstrate that Th2 cells have a profound effect on ILC2 expansion, which is redundantly mediated by IL-25 and IL-33.

IL-4 is critical for the induction of type 2 alarmins by Th2 cells

ILC2 expansion induced by chronic papain challenges in the *Il4/Il13*$^{-/-}$ mice was significantly reduced compared with the WT mice (Figures S6A and S6B). Furthermore, such reduction was observed in the *Il4*$^{-/-}$ mice, suggesting that IL-4 itself plays an important role (Figures S6C and S6D). To minimize the effect of IL-4 during *in vivo* Th2 cell differentiation, which may indirectly affect type 2 alarmin induction and thus ILC2 cell expansion, we treated the mice that received WT OT-II *in-vitro*-differentiated Th2 cells with an anti-IL-4 neutralizing antibody (Figure 6A) and found that IL-4 neutralization significantly reduced the amounts of all type 2 alarmins in the BALF fluid (Figure 6B). Furthermore, IL-4 neutralization also reduced eosinophilia and limited ILC2 expansion and activation (Figure 6C).

To test whether IL-4 is sufficient to induce ILC2-mediated type 2 responses, we challenged naive mice i.n. with IL-4 and IL-13 for 6 consecutive days (Figure 6D). Mice challenged with IL-4 showed a significant increase of eosinophils in the BALF accompanied by increased ILC2 cell number and their enhanced ability to produce IL-5 and IL-13 (Figure 6E, top panel). On the other hand, mice that received IL-13 showed much less eosinophilia and ILC2 activation compared with IL-4-treated mice, suggesting that IL-4 is the key

cytokine in mediating feedback from Th2 cells to ILC2s. A similar result was obtained using the *Rag1*$^{-/-}$ mice (Figure 6E, bottom panel), indicating that the IL-4 effect on ILC2s bypasses the need for Th2 cells. Furthermore, IL-4, but not IL-13, treatment significantly induced the expression of IL-33 and TSLP (Figure 6F, top panel). Similar regulation of type 2 alarmin expression by IL-4 was also observed in the *Rag1*$^{-/-}$ mice (Figure 6F, bottom panel).

To test the role of ILC2s in mediating IL-4-induced eosinophilia, we compared WT (*Gata3*$^{fl/fl}$) and ILC2-deficient (*Klrg1*^{Cre}*Gata3*$^{fl/fl}$) mice in response to IL-4 i.n. challenges. The results showed that ILC2-deficient mice did not develop eosinophilia (Figure 6G), indicating that ILC2s are critical for inducing eosinophilia in response to IL-4-induced type 2 alarmins. IL-4 has been reported to directly activate ILC2s.[41] To assess the importance of type 2 alarmins in activating ILC2s in this IL-4 challenge model, we tested the IL-33 trap and *Crlf2*$^{-/-}$ mice. While both WT and *Crlf2*$^{-/-}$ mice elicited similar levels of eosinophils in the BALF and equivalent ILC2 expansion in the lung tissue (Figure 6H), the IL-33 trap mice failed to show eosinophilia in response to IL-4 i.n. challenges, with no obvious ILC2 expansion and activation (Figure 6I). These data indicate that IL-4 induces ILC2 expansion and activation largely through upregulating type 2 alarmins.

ILC2s and Th2 cells function at different stages of host defense against *N. brasiliensis* infection

Nippostrongylus brasiliensis (*N. brasiliensis*) is a murine gastrointestinal parasite whose virulent L3 stage larvae complete part of their life cycle in the lung (L4 stage) before they migrate to the intestine to mature into adult worms (L5 stage). The adult worm has a reproductive life cycle in the intestine to produce eggs. Eggs produced by adult worms in the intestine are excreted through the fecal matter.[37] Infection with L3 stage larvae elicits a strong type 2 immunity; however, the role of ILC2s in host defense against *N. brasiliensis* infection and their functions in inducing Th2 responses are still controversial, and it is unknown whether Th2 cells are necessary for the sustained activation and functions of ILC2s during infection.

Both Th2 cells and ILC2s are capable of producing type 2 cytokines; however, it has been reported that ILC2s are poor IL-4-producing cells. Indeed, in response to *N. brasiliensis* infection, ILC2s showed significantly higher IL-13-producing capacity than Th2 cells (Figure S7A). By contrast, Th2 cells preferentially express IL-4 relative to ILC2s (Figure S7B).

To investigate the crosstalk between ILC2s and Th2 cells during *N. brasiliensis* infection, we infected the WT (*Gata3*$^{fl/fl}$), Th2-deficient (h*CD2*^{Cre}*Gata3*$^{fl/fl}$), and ILC2-deficient (*Klrg1*^{Cre} *Gata3*$^{fl/fl}$) mice with 500 virulent L3 stage larvae. The egg count was monitored daily throughout the infection, whereas worm burden and immune responses at the cellular level were measured on days 0, 7, 11, and 15 post-infection (Figure 7A). Egg counts revealed that all mice in different groups started excreting eggs 5 days post-infection (dpi) (Figure 7B). While egg release from *Gata3*$^{fl/fl}$ mice reached the peak level on 7 dpi and stopped completely on 10 dpi, both *Klrg1*^{Cre}*Gata3*$^{fl/fl}$ mice and h*CD2*^{Cre}*Gata3*$^{fl/fl}$ mice excreted more eggs than *Gata3*$^{fl/fl}$ mice starting from 7 dpi and had a maximum production on 10 dpi.

While the egg release started to reduce on 11 dpi and stopped on 14 dpi in *Klrg1*^{Cre}*Gata3*$^{fl/fl}$ mice, h*CD2*^{Cre}*Gata3*$^{fl/fl}$ mice continuously released high numbers of eggs in the fecal matter.

The enumeration of adult worms in the small intestine demonstrated that the numbers of adult worms in the intestine correlated well with the egg counts (Figure 7C). Seven days after infection, *Klrg1*^{Cre}*Gata3*$^{fl/fl}$ mice had higher worm burden than *Gata3*$^{fl/fl}$ and h*CD2*^{Cre}*Gata3*$^{fl/fl}$ mice, indicating that ILC2s are required for early host defense against helminth infection. Eleven days after infection, when *Gata3*$^{fl/fl}$ mice had completely expelled the worms, *Klrg1*^{Cre}*Gata3*$^{fl/fl}$ and h*CD2*^{Cre}*Gata3*$^{fl/fl}$ mice still had a high worm burden. Notably, while *Klrg1*^{Cre}*Gata3*$^{fl/fl}$ mice expelled worms by 15 dpi, h*CD2*^{Cre}*Gata3*$^{fl/fl}$ mice failed to expel worms (Figure 7C).

To test whether Th2 cells are absolutely required for worm expulsion, we monitored egg production in infected mice for a prolonged period of time. The results showed that egg production from the infected h*CD2*^{Cre}*Gata3*$^{fl/fl}$ mice started to reduce 15 dpi, and no eggs were detected after 28 dpi (Figure 7D). In addition, while WT mice and *Rag1*$^{-/-}$ mice stopped releasing eggs on 10 and 30 dpi, respectively, the *Rag2*$^{-/-}$*Il2rg*$^{-/-}$ mice continued to release eggs even after 150 days (Figure 7E). These data indicate that ILC2s may play an important role in worm expulsion in the absence of Th2 cells.

Crosstalk between ILC2s and Th2 cells during *N. brasiliensis* infection

To better understand the type 2 immune response to *N. brasiliensis* infection in the absence of ILC2s or Th2 cells, we measured the numbers of eosinophils, ILC2s, and Th2 cells in the BALF, lung, mediastinal lymph node, and mesenteric lymph node. A milder eosinophilia was observed in the BALF and lung tissues of the *Klrg1*^{Cre}*Gata3*$^{fl/fl}$ and h*CD2*^{Cre}*Gata3*$^{fl/fl}$ mice throughout the infection compared with the *Gata3*$^{fl/fl}$ mice (Figure 7F). Notably, while Th2 cells in the lungs and mediastinal lymph nodes were fewer in the *Klrg1*^{Cre}*Gata3*$^{fl/fl}$ mice than that in the *Gata3*$^{fl/fl}$ mice on day 11 (Figure 7G), more Th2 cells in the mesenteric lymph nodes of the *Klrg1*^{Cre}*Gata3*$^{fl/fl}$ mice were detected compared with *Gata3*$^{fl/fl}$ mice on days 11 and 15 (Figure 7G). These results indicate that Th2 cell differentiation does not require ILC2s. However, ILC2s may promote and/or accelerate this process.

Similarly, fewer numbers of ILC2s in the lung, mediastinal lymph node, and mesenteric lymph node were detected in the h*CD2*^{Cre}*Gata3*$^{fl/fl}$ mice compared with the *Gata3*$^{fl/fl}$ mice, especially on day 11 post-infection (Figure 7H). Although similar numbers of ILC2s were found in both groups of mice on day 15, by then, the *Gata3*$^{fl/fl}$ mice had already expelled the worms, and thus the type 2 immune response was probably in the contraction phase. The contraction phase of the immune responses between day 11 and 15 was supported by the reduction of both Th2 cells and ILC2s in the WT mice. Overall, we demonstrated that there is a crosstalk between ILC2s and Th2 cells during *N. brasiliensis* infection.

DISCUSSION

The relative contributions of Th2 cells and ILC2s, as well as crosstalk between these cells, particularly on how Th2 cells influence ILC2s, during *in vivo* type 2 immune responses

are still controversial and incompletely understood.[18,21,23,42] ILC2s and Th2 cells share the common hallmark transcription factor GATA3 for their development, maintenance, and functions.[14,17,43–46] Because of the essential role of GATA3 in these cells, it is an ideal target for creating ILC2- or Th2-deficient animal models. Based on the preferential expression pattern of certain molecules in ILCs (i.e., KLRG1 for ILC2s) and T cells, we took advantage of the Cre-loxP system in deleting the *Gata3* gene in either ILC2s or mature T cells. Specifically, we generated the $Klrg1^{Cre}Gata3^{fl/fl}$ mice that are deficient in ILC2s but not Th2 cells and the h$CD2^{Cre}Gata3^{fl/fl}$ mice that fail to generate Th2 cells, yet ILC2s in these mice are intact. By using these mouse strains, we systematically assessed the functions of ILC2s and Th2 cells, and their crosstalk in a variety of type 2 immune response models.

ILC2-independent Th2 cell differentiation can occur in response to OVA/alum immunization. However, ILC2s may promote Th2 cell responses in other settings, including in the papain-induced type 2 immune response at the chronic stage. During helminth infection, although Th2 cell differentiation seemed to be delayed, we did observe Th2 cell differentiation in the absence of ILC2s, consistent with a previous report.[23] These results indicate that Th2 cell differentiation itself does not require ILC2s. However, whenever ILC2s are activated by type 2 alarmins, they could potentiate and/or promote Th2 cell responses.

In all the models that we have tested, Th2 cells can expand the total numbers of ILC2s, and the expansion of ILC2s is diminished in either $Rag1^{-/-}$ or Th2-deficient mice. Such ILC2 expansion is correlated with the induction of type 2 alarmin expression. Th2 cells are necessary and sufficient for promoting the expression of type 2 alarmins. We also show that the induction of IL-25, IL-33, and TSLP expression by Th2 cells was IL-4 dependent. Furthermore, IL-4 was sufficient to induce IL-33 and TSLP in the absence of T cells. The fact that IL-4 was required for IL-25 induction but not sufficient for inducing IL-25 implies that other Th2 molecules and/or cell-cell interaction, in addition to IL-4, may be required for regulating IL-25 expression.

Interestingly, while blocking signaling of individual type 2 alarmins has no significant effect on ILC2 expansion, blocking both IL-25 and IL-33 severely hampers Th2 cell-induced ILC2 expansion. Thus, Th2 cells can indirectly influence the expansion of ILC2s through promoting the release of type 2 alarmins, among which IL-25 and IL-33 play a redundant role. By contrast, TSLP has a minimal effect if any on activating ILC2s, although it plays an important role in the Th2 cell response induced by OVA/alum immunization. It has been reported that IL-25 produced by tuft cells mediates a positive feedback loop between type 2 lymphocytes and tuft cells in the gut.[47] Our results further expand this notion that crossregulation between type 2 effector cytokines and alarmins may mediate the crosstalk between Th2 cells and ILC2s. However, depending on the amounts of IL-33 and IL-25 that can be induced in different tissues, these alarmins may play a redundant role. The non-redundant function of IL-25 in mediating Th2-ILC2-tuft cell crosstalk in the gut is possibly due to its relative abundance in the gut tissue and the lack of IL-33 receptor expression by gut ILC2s.

The crosstalk between ILC2s and Th2 cells was also observed in a helminth *N. brasiliensis* infection model. It has been shown that ILC2 deficiency may impair the host's ability to clear worms and that transferring ILC2s rescues such a defect.[42] On the other hand, transferring T cells into either ILC2-sufficient or ILC2-deficient mice on the *Rag1*$^{-/-}$ background results in an equally efficient worm expulsion.[23] However, in both cases, it might be difficult to determine whether the transferred cells truly behave as endogenous ILC2s or Th2 cells under physiological conditions. In fact, expansion of ILC2s in *Rag*$^{-/-}$ mice via cytokine injection is sufficient to expel worms.[18,48] Consistent with a previous report,[49] our results strongly suggest that ILC2s and Th2 cells function at the different stages of host defense during helminth infection. While our article was under final review, another study reported that ILC2s have a non-redundant function in worm expulsion.[50] However, this conclusion was largely based on their result, similar to our observation, that on day 11, when the WT mice completely expelled the worms, the worms were still present in the ILC2-deficient mice. We further demonstrated that on day 15, our ILC2-deficient mice were able to expel worms; whether this is also the case with the other recently generated ILC2-deficient mouse strain remains to be tested. Nevertheless, our current study indicates that ILC2s play an important role at an early stage and that without ILC2s, worm expulsion is delayed. On the other hand, Th2 cells function at a relatively late stage even in the absence of ILC2s. Conversely, in the absence of Th2 cells, ILC2s alone can still expel worms but with a long delay. Thus, while ILC2s and Th2 cells function at different stages, they have overlapping functions and can cooperate to mount an efficient immune response against helminth infection.

In summary, our results indicate that ILC2s and Th2 cells have a mutual crosstalk while establishing and executing an effective and robust type 2 immune response. Initial activation of the ILC2s by type 2 alarmins may promote Th2 cell differentiation, although ILC2-independent Th2 cell differentiation also occurs. Th2 cells, in turn, may induce the production of type 2 alarmins to promote the expansion of ILC2s. Thus, the relative importance of ILC2s and Th2 cells during a type 2 immune response may depend on the timing, the tissue distribution of these type 2 lymphocytes, and the nature of the extrinsic signals that activate these cells. Our notion of model-dependent crosstalk between ILC2s and Th2 cells during type 2 immune responses may help to explain mechanisms underlying different forms of human allergic inflammatory disorders and helminth infections.

Limitations of the study

While we have shown that IL-4 was important for Th2 cell-mediated alarmin expression, the target cells for IL-4 were not investigated in this study. For the mouse models, although Th2 cells are not significantly affected by *Klrg1*^{Cre}-mediated *Gata3* deletion, the subset of KLRG1-expressing Tregs could be defective in our ILC2-deficient mice. Nevertheless, this limitation should not alter the conclusions of our current study since, unlike ILC2s, Tregs usually limit rather than promote Th2 cell responses. *Klrg1*^{Cre} is also active in effector CD8^{+} T cells and NK subsets; thus, for investigating the role of ILC2s during viral infections, our ILC2-deficient mice should be used with caution because activated CD8^{+} effector T cells and a portion of NK cells would be GATA3 deficient in these settings.

STAR⋆METHODS

RESOURCE AVAILABILITY

Lead contact—Further information and requests for resources and reagents should be directed to and will be fulfilled by the lead contact, Jinfang Zhu (jfzhu@niaid.nih.gov).

Materials availability—*Klrg1*^{Cre}*Gata3*$^{fl/fl}$ (ILC2-deficient) and h*CD2*^{Cre}*Gata3*$^{fl/fl}$ (Th2-deficient) mouse strains are generated in this study.

Data and code availability

- The RNA-Seq datasets have been deposited and are now publicly available at the Gene Expression Omnibus database under the accession no. GSE166779, which is also listed in the key resources table.
- This paper does not report original code.
- Any additional information required to reanalyze the data reported in this paper is available from the lead contact upon request.

EXPERIMENTAL MODEL AND SUBJECT DETAILS

The *Klrg1*^{Cre} mice[27] on C57BL/6 background, kindly provided by Dr. Richard Flavell of Yale University, were bred to *Gata3*$^{fl/fl}$ mice[14] to generate *Klrg1*^{Cre}*Gata3*$^{fl/fl}$ (ILC2-deficient) mice. The h*CD2*^{Cre}*Gata3*$^{fl/fl}$ (Th2-deficient) mice were generated by crossing *Gata3*$^{fl/fl}$ mice with h*CD2*^{Cre} mice,[51] kindly provided by Dr. Paul Love of NICHD (now also available as Stock No: 027406 at the Jackson Laboratories). The CIKS KO mice (line 290),[34] *Il4/Il13*$^{-/-}$ mice (line 242), *Il4*$^{-/-}$ mice (line 46) and OT-II (line 361) were obtained from the NIAID-Taconic repository. TSLPR KO (*Crlf2*$^{-/-}$) mice were previously reported.[36] IL-33-trap mouse strain[35] was kindly provided by late Dr. William E. Paul of NIAID. Mice were bred and/or maintained in the NIAID specific pathogen-free animal facilities. Both female and male mice were used for experiments. Mice in each experimental group were sex and age matched (8–12 wk). All the animal studies were carried out under a protocol approved by the National Institute of Allergy and Infectious Diseases (NIAID) Animal Care and Use Committee.

For genotyping, tail or ear pinna samples were incubated with lysis buffer (100 mM Tris-HCl, pH 8.5, 5 mM EDTA, 0.2% SDS, 200 mM NaCl and 1 mg/mL of proteinase K) overnight at 55°C overnight, followed by a 1:10 dilution with distilled water and 1 μL was then used as template for PCR. The genotyping of *Klrg1*^{Cre},[27] *Crlf2*$^{-/-}$,[36] IL-33-trap,[35] and *Gata3*$^{fl/fl}$ mice[14] was performed as previously described.

METHOD DETAILS

T helper cell differentiation *in vitro*—Naive CD4^{+} T cells were enriched from peripheral lymph nodes with naive CD4^{+} T cell isolation kit according to the manufacturer instruction (STEMCELL Technologies). Enriched cells were cultured for 4 days under Th1 polarizing conditions (anti-CD3, 1 μg/mL, anti-CD28, 3 μg/mL, anti-IL-4, 10 μg/mL, IL-12, 10 ng/mL, IL-2, 100 U/mL), Th2 polarizing conditions (anti-CD3, 1 μg/mL, anti-CD28, 3

μg/mL, anti-IFN-γ, 10 μg/mL, anti-IL-12, 10 μg/mL, IL-4, 10 ng/mL, IL-2, 100 U/mL), and Th17 polarizing conditions (anti-CD3, 1 μg/mL, anti-CD28, 3 μg/mL, anti-IFN-γ, 10 μg/mL, anti-IL-4, 10 μg/mL, anti-IL-12, 10 μg/mL, TGFβ, 1 ng/mL, IL-6, 10 ng/mL, IL-1β, 10 ng/mL). Mitomycin-C treated T-depleted splenocytes were used as APCs at 5:1 ratio. Differentiated cells were re-stimulated with PMA/ionomycin for cytokine expression analysis.

Generation of OVA-specific Th2 cells *in vitro*—Naive OT-II-CD4$^+$ T (CD4$^+$CD44$^-$CD25$^-$) cells were enriched from peripheral lymph nodes and spleen with naive CD4$^+$ T cell isolation kit according to the manufacturer instruction (Miltenyi Biotech). Enriched cells were cultured under Th2 conditions (Dynabeads mouse T activator CD3/CD28, 12 μL/mL; IL-4, 20 ng/mL; anti-IFN-γ, 10 μg/mL; anti-IL-12, 10 μg/mL; IL-2, 100 U/mL) for 4 days. Later, the Dynabeads were separated from the culture by passing through LS columns (Miltenyi Biotech). Effector Th2 cells were cultured in the RPMI 1640 medium supplemented with 10% FBS and hIL-2 (100 U/mL) for 3 days before injecting into the mice.

Mouse models of airway inflammation—For protease papain induced airway inflammation, mice were anesthetized with isoflurane and 40 μg of papain (in 20 μL of PBS) was intranasally (*i.n.*) administrated into mice on day 0, 1, and 2. Mice were either sacrificed on day 3 for acute studies or rested for 10 days before challenged with papain on day 13, 14 and 15 for chronic studies.

For OVA-induced airway inflammation, mice were immunized with intraperitoneal (*i.p.*) injection of 20 μg of OVA emulsified in Imject Alum (1:3) in 100 μL of PBS on day 0, and booster on day 7. Mice injected only with Imject Alum were considered as the PBS control group. After four days these mice were intranasally challenged with 20 μL OVA (2 mg/mL) on day 11, 12, 13 and 14.

For adoptive cell transfer induced airway inflammation, *Rag1*$^{-/-}$ or C57BL/6 mice intranasally administrated with 20 μL of OVA (2 mg/mL) one day before one million of *in vitro*-differentiated OT-II Th2 cells were injected intravenously (*i.v.*) into these mice. The mice were further challenged with intranasally with OVA on day 1, 2, 3, 4, and 5.

For IL-4-induced airway inflammation, mice were anesthetized with isoflurane and *i.n.* challenged with 1 μg IL-4 or IL-13 for 6 consecutive days.

In all these models, mice were sacrificed 24 h after the final *i.n.* challenge. BAL fluid, lungs, and mediastinal lymph nodes were analyzed.

ILC2 activation *in vitro*—The lung cell suspension from WT mice was prepared as described above. The prepared lung suspension was stained with viability dye, lineage markers, CD127, and T1/ST2. The ILC2s were purified by gating on live lineage$^-$CD127$^+$T1ST2$^+$ cells. Sorted ILC2s were then cultured in 96 well U bottom plates in RPMI1640 + 10% FBS with TSLP (40 ng/mL), IL-25 (10 ng/mL), or IL-33 (10 ng/mL)

along with IL-2 (100 U/mL) and IL-7 (10 ng/mL) for 3 days. Cells were then stimulated with PMA/ionomycin and stained for IL-5 and IL-13 expression.

***N. brasiliensis* infection—**Mice were subcutaneously inoculated with 500 infective third-stage larvae (L3) of *N. brasiliensis*. The enumeration of eggs in the feces and adult worms in the intestine was performed as previously described.[37]

Cell preparation and flow cytometry analysis—BALF was obtained by flushing lung twice with 0.8 mL of PBS using a syringe cannula. The lung lobes were chopped into small pieces and digested with collagenase type IV (1 mg/mL) and DNase I (100 U/mL) in plain PBS for 20 min at 37°C. The digestion was terminated by adding ice-cold RPMI 1640 + 10% FBS, then the entire digested tissue was mashed through 40μm cell strainer to obtain single cell suspension. ACK lysis buffer was used to lyse RBCs in BALF and lung cell suspension.

Cells obtained from BALF, lung and lymph nodes were stained with different antibody cocktails for identifying eosinophils, Th2 cells, and ILC2s and then analyzed by FACS LSR-II or Fortessa (BD Bioscience). Intracellular staining was performed by using Foxp3/transcription factor staining buffer set (eBioscience). Eosinophils were identified as $CD45^+CD11c^-Gr1^-Siglec\ F^+CD11b^+$; Th2 cells were identified as $CD45^+CD4^+Foxp3^-GATA3^+T1/ST2^+$; ILC2s were identified as $CD45^+Lin^-IL\text{-}7R\alpha^+GATA3^+T1/ST2^+$. All flow cytometric data analysis was performed on FlowJo software (BD Bioscience).

ELISA

IL-25, IL-33, and TSLP levels in the BALF were measured by ELISA Kits (Cat# DY1399, DY3626, and MTLP00; R&D Biosystem). All the procedures were performed according to the manufacturers' instructions. Briefly, ELISA plates were coated with the appropriate concentration of specific primary antibody in PBS overnight at 4°C. The plates were then blocked for 1 h to eliminate nonspecific binding before they were incubated with isolated BALF samples or appropriate standards for 2 h. These plates were incubated for another 2 h with appropriate biotin-conjugated secondary antibody, followed by streptavidin-HRP. Each step was followed by an appropriate number of washings with PBS buffer +0.05% Tween 20. The plates were developed with the TMB substrate solution (Cat# 421101; Biolegend). The stop solution for TMB substrate (Cat# 423001; Biolegend) was used to terminate the reaction. Final absorbance was measured at 450 nm. The concentration of cytokines in the BALF was calculated based on the standard curve fitting method with GrapPad Prism.

Histological analysis of lung tissue—Lung sections were prepared and analyzed by Histoserve, Inc (Germantown, MD). Briefly, after cardiac perfusion, lungs were removed and fixed in 10% buffered formaldehyde and stored. The lung tissue was paraffin-embedded, and sections were stained with H&E or periodic acid-Schiff (PAS) for the quantification of cellular infiltration and bronchial mucus gland hypertrophy. The severity of inflammation was analyzed by blinded histopathological scoring.

T cell transfer-mediated colitis model—Naive $CD4^+$ T cells from pooled lymph nodes and spleen of the *Gata3*$^{fl/fl}$ mice or *hCD2*^{Cre}*Gata3*$^{fl/fl}$ mice were sorted as the live $CD4^+CD45RB^{hi}CD25^-$ population. To induce colitis, *Rag1*$^{-/-}$ mice were injected *i.v.* with 300,000 naive $CD4^+$ T cells. Body weight of these mice was measured before transfer and every three days after transfer until they reduced 10% of their body weight. Mice were then euthanized and Th1 cells in the mesenteric lymph node were analyzed.

RNA-seq analysis—ILC2s (Lin^-IL-7Rα^+T1/$ST2^+$) from inflamed lung tissue after chronic papain challenges were sorted for RNA-Seq experiments. The RNA-Seq was performed as described previously.[52] Briefly, the total RNAs were harvested and purified by using Qiagen's RNeasy micro kit (74004; Qiagen). Qiagen's DNase set (79,254; Qiagen) was used for on-column DNase digestion. Poly A-tailed RNA was purified from total RNA by using Dynabeads mRNA DIRECT kit (61,012; Ambion Life Technologies). The libraries were sequenced with Illumina HiSeq system, and 50 bp reads were generated by the National Heart, Lung, and Blood Institute DNA Sequencing and Genomics Core. The RNA-Seq analysis was performed by Partek Flow. Briefly, the sequence reads were mapped to mouse genome (mm10) by using STAR with default settings. Read length ≤10 bp were discarded to eliminate the mapping to multiple positions. Partek E/M was used for the quantification of reads, and reads normalization was done by count per million reads. Differentially expressed genes were identified by using GSA method with the following criteria, p value ≤ 0.05, fold change ≤ −1.7 or ≥ 1.7.

QUANTIFICATION AND STATISTICAL ANALYSIS

Data analysis was performed with GraphPad Prism (GraphPad Software). Differences between two groups were determined by two-tailed unpaired or paired Student's *t*-test. Data were presented as mean ± SEM. A p value <0.05 was considered statistically significant and indicated as *; $p < 0.01$ was indicated as **; $p < 0.001$ was indicated as ***; and $p < 0.0001$ was indicated as ****. Not statistically significant was indicated as ns.

Supplementary Material

Refer to Web version on PubMed Central for supplementary material.

ACKNOWLEDGMENTS

We thank Ke Weng of NIAID for cell sorting and the NHLBI DNA Sequencing Core facility for sequencing the RNA-seq libraries. We thank Sundar Ganesan of the Biological Imaging Facility at the NIAID for bright-field images of histopathology samples. This work is supported by the Division of Intramural Research, NIAID, National Institutes of Health (grant 1ZIA-AI-001169) and the US-China Biomedical Collaborative Research Program (grant AI-129775). B.S. is supported by a grant from the National Natural Science Foundation of China (grant 81761128009).

REFERENCES

1. Fang D, and Zhu J (2017). Dynamic balance between master transcription factors determines the fates and functions of CD4 T cell and innate lymphoid cell subsets. J. Exp. Med 214, 1861–1876. 10.1084/jem.20170494. [PubMed: 28630089]

2. Diefenbach A, Colonna M, and Koyasu S (2014). Development, differentiation, and diversity of innate lymphoid cells. Immunity 41, 354–365. 10.1016/j.immuni.2014.09.005. [PubMed: 25238093]

3. Gurram RK, and Zhu J (2019). Orchestration between ILC2s and Th2 cells in shaping type 2 immune responses. Cell. Mol. Immunol 16, 225–235. 10.1038/s41423-019-0210-8. [PubMed: 30792500]

4. Walker JA, and McKenzie ANJ (2018). TH2 cell development and function. Nat. Rev. Immunol 18, 121–133. 10.1038/nri.2017.118. [PubMed: 29082915]

5. Ruterbusch M, Pruner KB, Shehata L, and Pepper M (2020). In vivo CD4(+) T cell differentiation and function: revisiting the Th1/Th2 paradigm. Annu. Rev. Immunol 38, 705–725. 10.1146/annurev-immunol-103019-085803. [PubMed: 32340571]

6. Ricardo-Gonzalez RR, Van Dyken SJ, Schneider C, Lee J, Nussbaum JC, Liang HE, Vaka D, Eckalbar WL, Molofsky AB, Erle DJ, and Locksley RM (2018). Tissue signals imprint ILC2 identity with anticipatory function. Nat. Immunol 19, 1093–1099. 10.1038/s41590-018-0201-4. [PubMed: 30201992]

7. Zhu J (2018). Mysterious ILC2 tissue adaptation. Nat. Immunol 19, 1042–1044. 10.1038/s41590-018-0214-z. [PubMed: 30201993]

8. Schneider C, Lee J, Koga S, Ricardo-Gonzalez RR, Nussbaum JC, Smith LK, Villeda SA, Liang HE, and Locksley RM (2019). Tissue-resident group 2 innate lymphoid cells differentiate by layered ontogeny and in situ perinatal priming. Immunity 50, 1425–1438.e5. 10.1016/j.immuni.2019.04.019. [PubMed: 31128962]

9. Martinez-Gonzalez I, Steer CA, and Takei F (2015). Lung ILC2s link innate and adaptive responses in allergic inflammation. Trends Immunol 36, 189–195. 10.1016/j.it.2015.01.005. [PubMed: 25704560]

10. Zheng W, and Flavell RA (1997). The transcription factor GATA-3 is necessary and sufficient for Th2 cytokine gene expression in CD4 T cells. Cell 89, 587–596. [PubMed: 9160750]

11. Zhang DH, Cohn L, Ray P, Bottomly K, and Ray A (1997). Transcription factor GATA-3 is differentially expressed in murine Th1 and Th2 cells and controls Th2-specific expression of the interleukin-5 gene. J. Biol. Chem 272, 21597–21603. [PubMed: 9261181]

12. Ouyang W, Ranganath SH, Weindel K, Bhattacharya D, Murphy TL, Sha WC, and Murphy KM (1998). Inhibition of Th1 development mediated by GATA-3 through an IL-4-independent mechanism. Immunity 9, 745–755. 10.1016/s1074-7613(00)80671-8. [PubMed: 9846495]

13. Pai SY, Truitt ML, and Ho IC (2004). GATA-3 deficiency abrogates the development and maintenance of T helper type 2 cells. Proc. Natl. Acad. Sci. USA 101, 1993–1998. [PubMed: 14769923]

14. Zhu J, Min B, Hu-Li J, Watson CJ, Grinberg A, Wang Q, Killeen N, Urban JF Jr., Guo L, and Paul WE (2004). Conditional deletion of Gata3 shows its essential function in T(H)1-T(H)2 responses. Nat. Immunol 5, 1157–1165. 10.1038/ni1128. [PubMed: 15475959]

15. Hoyler T, Klose CSN, Souabni A, Turqueti-Neves A, Pfeifer D, Rawlins EL, Voehringer D, Busslinger M, and Diefenbach A (2012). The transcription factor GATA-3 controls cell fate and maintenance of type 2 innate lymphoid cells. Immunity 37, 634–648. 10.1016/j.immuni.2012.06.020. [PubMed: 23063333]

16. Mjösberg J, Bernink J, Golebski K, Karrich JJ, Peters CP, Blom B, te Velde AA, Fokkens WJ, van Drunen CM, and Spits H (2012). The transcription factor GATA3 is essential for the function of human type 2 innate lymphoid cells. Immunity 37, 649–659. 10.1016/j.immuni.2012.08.015. [PubMed: 23063330]

17. Yagi R, Zhong C, Northrup DL, Yu F, Bouladoux N, Spencer S, Hu G, Barron L, Sharma S, Nakayama T, et al. (2014). The transcription factor GATA3 is critical for the development of all IL-7Ralpha-expressing innate lymphoid cells. Immunity 40, 378–388. 10.1016/j.immuni.2014.01.012. [PubMed: 24631153]

18. Oliphant CJ, Hwang YY, Walker JA, Salimi M, Wong SH, Brewer JM, Englezakis A, Barlow JL, Hams E, Scanlon ST, et al. (2014). MHCII-mediated dialog between group 2 innate lymphoid cells and CD4(+) T cells potentiates type 2 immunity and promotes parasitic helminth expulsion. Immunity 41, 283–295. 10.1016/j.immuni.2014.06.016. [PubMed: 25088770]

19. Halim TYF, Rana BMJ, Walker JA, Kerscher B, Knolle MD, Jolin HE, Serrao EM, Haim-Vilmovsky L, Teichmann SA, Rodewald HR, et al. (2018). Tissue-restricted adaptive type 2 immunity is orchestrated by expression of the costimulatory molecule OX40L on group 2 innate lymphoid cells. Immunity 48, 1195–1207.e6. 10.1016/j.immuni.2018.05.003. [PubMed: 29907525]
20. Schwartz C, Khan AR, Floudas A, Saunders SP, Hams E, Rodewald HR, McKenzie ANJ, and Fallon PG (2017). ILC2s regulate adaptive Th2 cell functions via PD-L1 checkpoint control. J. Exp. Med 214, 2507–2521. 10.1084/jem.20170051. [PubMed: 28747424]
21. Halim TYF, Steer CA, Mathä L, Gold MJ, Martinez-Gonzalez I, McNagny KM, McKenzie ANJ, and Takei F (2014). Group 2 innate lymphoid cells are critical for the initiation of adaptive T helper 2 cell-mediated allergic lung inflammation. Immunity 40, 425–435. 10.1016/j.immuni.2014.01.011. [PubMed: 24613091]
22. Halim TYF, Hwang YY, Scanlon ST, Zaghouani H, Garbi N, Fallon PG, and McKenzie ANJ (2016). Group 2 innate lymphoid cells license dendritic cells to potentiate memory TH2 cell responses. Nat. Immunol 17, 57–64. 10.1038/ni.3294. [PubMed: 26523868]
23. Van Dyken SJ, Nussbaum JC, Lee J, Molofsky AB, Liang HE, Pollack JL, Gate RE, Haliburton GE, Ye CJ, Marson A, et al. (2016). A tissue checkpoint regulates type 2 immunity. Nat. Immunol 17, 1381–1387. 10.1038/ni.3582. [PubMed: 27749840]
24. Mirchandani AS, Besnard AG, Yip E, Scott C, Bain CC, Cerovic V, Salmond RJ, and Liew FY (2014). Type 2 innate lymphoid cells drive CD4+ Th2 cell responses. J. Immunol 192, 2442–2448. 10.4049/jimmunol.1300974. [PubMed: 24470502]
25. Symowski C, and Voehringer D (2019). Th2 cell-derived IL-4/IL-13 promote ILC2 accumulation in the lung by ILC2-intrinsic STAT6 signaling in mice. Eur. J. Immunol 49, 1421–1432. 10.1002/eji.201948161. [PubMed: 31144294]
26. Wang JM, Cheng YQ, Shi L, Ying RS, Wu XY, Li GY, Moorman JP, and Yao ZQ (2013). KLRG1 negatively regulates natural killer cell functions through the Akt pathway in individuals with chronic hepatitis C virus infection. J. Virol 87, 11626–11636. 10.1128/JVI.01515-13. [PubMed: 23966413]
27. Herndler-Brandstetter D, Ishigame H, Shinnakasu R, Plajer V, Stecher C, Zhao J, Lietzenmayer M, Kroehling L, Takumi A, Kometani K, et al. (2018). KLRG1(+) effector CD8(+) T cells lose KLRG1, differentiate into all memory T cell lineages, and convey enhanced protective immunity. Immunity 48, 716–729.e8. 10.1016/j.immuni.2018.03.015. [PubMed: 29625895]
28. Nussbaum JC, Van Dyken SJ, von Moltke J, Cheng LE, Mohapatra A, Molofsky AB, Thornton EE, Krummel MF, Chawla A, Liang HE, and Locksley RM (2013). Type 2 innate lymphoid cells control eosinophil homeostasis. Nature 502, 245–248. 10.1038/nature12526. [PubMed: 24037376]
29. Halim TYF, Krauss RH, Sun AC, and Takei F (2012). Lung natural helper cells are a critical source of Th2 cell-type cytokines in protease allergen-induced airway inflammation. Immunity 36, 451–463. 10.1016/j.immuni.2011.12.020. [PubMed: 22425247]
30. Sharma A, and Rudra D (2018). Emerging functions of regulatory T cells in tissue homeostasis. Front. Immunol 9, 883. 10.3389/fimmu.2018.00883. [PubMed: 29887862]
31. Wang Y, Su MA, and Wan YY (2011). An essential role of the transcription factor GATA-3 for the function of regulatory T cells. Immunity 35, 337–348. 10.1016/j.immuni.2011.08.012. [PubMed: 21924928]
32. Wohlfert EA, Grainger JR, Bouladoux N, Konkel JE, Oldenhove G, Ribeiro CH, Hall JA, Yagi R, Naik S, Bhairavabhotla R, et al. (2011). GATA3 controls Foxp3(+) regulatory T cell fate during inflammation in mice. J. Clin. Invest 121, 4503–4515. 10.1172/JCI57456. [PubMed: 21965331]
33. Moon JJ, Chu HH, Pepper M, McSorley SJ, Jameson SC, Kedl RM, and Jenkins MK (2007). Naive CD4(+) T cell frequency varies for different epitopes and predicts repertoire diversity and response magnitude. Immunity 27, 203–213. 10.1016/j.immuni.2007.07.007. [PubMed: 17707129]
34. Claudio E, Sønder SU, Saret S, Carvalho G, Ramalingam TR, Wynn TA, Chariot A, Garcia-Perganeda A, Leonardi A, Paun A, et al. (2009). The adaptor protein CIKS/Act1 is essential for IL-25-mediated allergic airway inflammation. J. Immunol 182, 1617–1630. 10.4049/jimmunol.182.3.1617. [PubMed: 19155511]

35. Pichery M, Mirey E, Mercier P, Lefrancais E, Dujardin A, Ortega N, and Girard JP (2012). Endogenous IL-33 is highly expressed in mouse epithelial barrier tissues, lymphoid organs, brain, embryos, and inflamed tissues: in situ analysis using a novel Il-33-LacZ gene trap reporter strain. J. Immunol 188, 3488–3495. 10.4049/jimmunol.1101977. [PubMed: 22371395]

36. Al-Shami A, Spolski R, Kelly J, Fry T, Schwartzberg PL, Pandey A, Mackall CL, and Leonard WJ (2004). A role for thymic stromal lymphopoietin in CD4(+) T cell development. J. Exp. Med 200, 159–168. [PubMed: 15263024]

37. Camberis M, Le Gros G, and Urban J Jr. (2003). Animal model of Nippostrongylus brasiliensis and Heligmosomoides polygyrus. Curr. Protoc. Im Chapter 19, Unit 19.12. 10.1002/0471142735.im1912s55.

38. Morita H, Arae K, Unno H, Miyauchi K, Toyama S, Nambu A, Oboki K, Ohno T, Motomura K, Matsuda A, et al. (2015). An interleukin-33-mast cell-interleukin-2 Axis suppresses papain-induced allergic inflammation by promoting regulatory T cell numbers. Immunity 43, 175–186. 10.1016/j.immuni.2015.06.021. [PubMed: 26200013]

39. Salimi M, Barlow JL, Saunders SP, Xue L, Gutowska-Owsiak D, Wang X, Huang LC, Johnson D, Scanlon ST, McKenzie ANJ, et al. (2013). A role for IL-25 and IL-33-driven type-2 innate lymphoid cells in atopic dermatitis. J. Exp. Med 210, 2939–2950. 10.1084/jem.20130351. [PubMed: 24323357]

40. Kim BS, Siracusa MC, Saenz SA, Noti M, Monticelli LA, Sonnenberg GF, Hepworth MR, Van Voorhees AS, Comeau MR, and Artis D (2013). TSLP elicits IL-33-independent innate lymphoid cell responses to promote skin inflammation. Sci. Transl. Med 5, 170ra16. 10.1126/scitranslmed.3005374.

41. Motomura Y, Morita H, Moro K, Nakae S, Artis D, Endo TA, Kuroki Y, Ohara O, Koyasu S, and Kubo M (2014). Basophil-derived interleukin-4 controls the function of natural helper cells, a member of ILC2s, in lung inflammation. Immunity 40, 758–771. 10.1016/j.immuni.2014.04.013. [PubMed: 24837103]

42. Yang Q, Monticelli LA, Saenz SA, Chi AWS, Sonnenberg GF, Tang J, De Obaldia ME, Bailis W, Bryson JL, Toscano K, et al. (2013). T cell factor 1 is required for group 2 innate lymphoid cell generation. Immunity 38, 694–704. 10.1016/j.immuni.2012.12.003. [PubMed: 23601684]

43. Zhou L (2012). Striking similarity: GATA-3 regulates ILC2 and Th2 cells. Immunity 37, 589–591. 10.1016/j.immuni.2012.10.002. [PubMed: 23084352]

44. Zhu J (2017). GATA3 regulates the development and functions of innate lymphoid cell subsets at multiple stages. Front. Immunol 8, 1571. 10.3389/fimmu.2017.01571. [PubMed: 29184556]

45. Moro K, Yamada T, Tanabe M, Takeuchi T, Ikawa T, Kawamoto H, Furusawa JI, Ohtani M, Fujii H, and Koyasu S (2010). Innate production of T(H)2 cytokines by adipose tissue-associated c-Kit(+)Sca-1(+) lymphoid cells. Nature 463, 540–544. 10.1038/nature08636. [PubMed: 20023630]

46. Spits H, and Cupedo T (2012). Innate lymphoid cells: emerging insights in development, lineage relationships, and function. Annu. Rev. Immunol 30, 647–675. 10.1146/annurev-immunol-020711-075053. [PubMed: 22224763]

47. von Moltke J, Ji M, Liang HE, and Locksley RM (2016). Tuft-cell-derived IL-25 regulates an intestinal ILC2-epithelial response circuit. Nature 529, 221–225. 10.1038/nature16161. [PubMed: 26675736]

48. Fallon PG, Ballantyne SJ, Mangan NE, Barlow JL, Dasvarma A, Hewett DR, McIlgorm A, Jolin HE, and McKenzie ANJ (2006). Identification of an interleukin (IL)-25-dependent cell population that provides IL-4, IL-5, and IL-13 at the onset of helminth expulsion. J. Exp. Med 203, 1105–1116. [PubMed: 16606668]

49. Wong SH, Walker JA, Jolin HE, Drynan LF, Hams E, Camelo A, Barlow JL, Neill DR, Panova V, Koch U, et al. (2012). Transcription factor RORalpha is critical for nuocyte development. Nat. Immunol 13, 229–236. 10.1038/ni.2208. [PubMed: 22267218]

50. Jarick KJ, Topczewska PM, Jakob MO, Yano H, Arifuzzaman M, Gao X, Boulekou S, Stokic-Trtica V, Leclère PS, Preußer A, et al. (2022). Non-redundant functions of group 2 innate lymphoid cells. Nature 611, 794–800. 10.1038/s41586-022-05395-5. [PubMed: 36323785]

51. Vacchio MS, Wang L, Bouladoux N, Carpenter AC, Xiong Y, Williams LC, Wohlfert E, Song KD, Belkaid Y, Love PE, and Bosselut R (2014). A ThPOK-LRF transcriptional node maintains

the integrity and effector potential of post-thymic CD4+ T cells. Nat. Immunol 15, 947–956. 10.1038/ni.2960. [PubMed: 25129370]

52. Fang D, Cui K, Hu G, Gurram RK, Zhong C, Oler AJ, Yagi R, Zhao M, Sharma S, Liu P, et al. (2018). Bcl11b, a novel GATA3-interacting protein, suppresses Th1 while limiting Th2 cell differentiation. J. Exp. Med 215, 1449–1462. 10.1084/jem.20171127. [PubMed: 29514917]

Highlights

- IL-33-mediated ILC2 activation promotes the pulmonary Th2 cell response to papain
- Th2 cell response to OVA immunization is ILC2 independent but TSLP dependent
- IL-25 and IL-33 are redundantly important in Th2 cell-mediated ILC2 expansion
- IL-4 is necessary for Th2 cell-mediated induction of IL-33 and TSLP expression

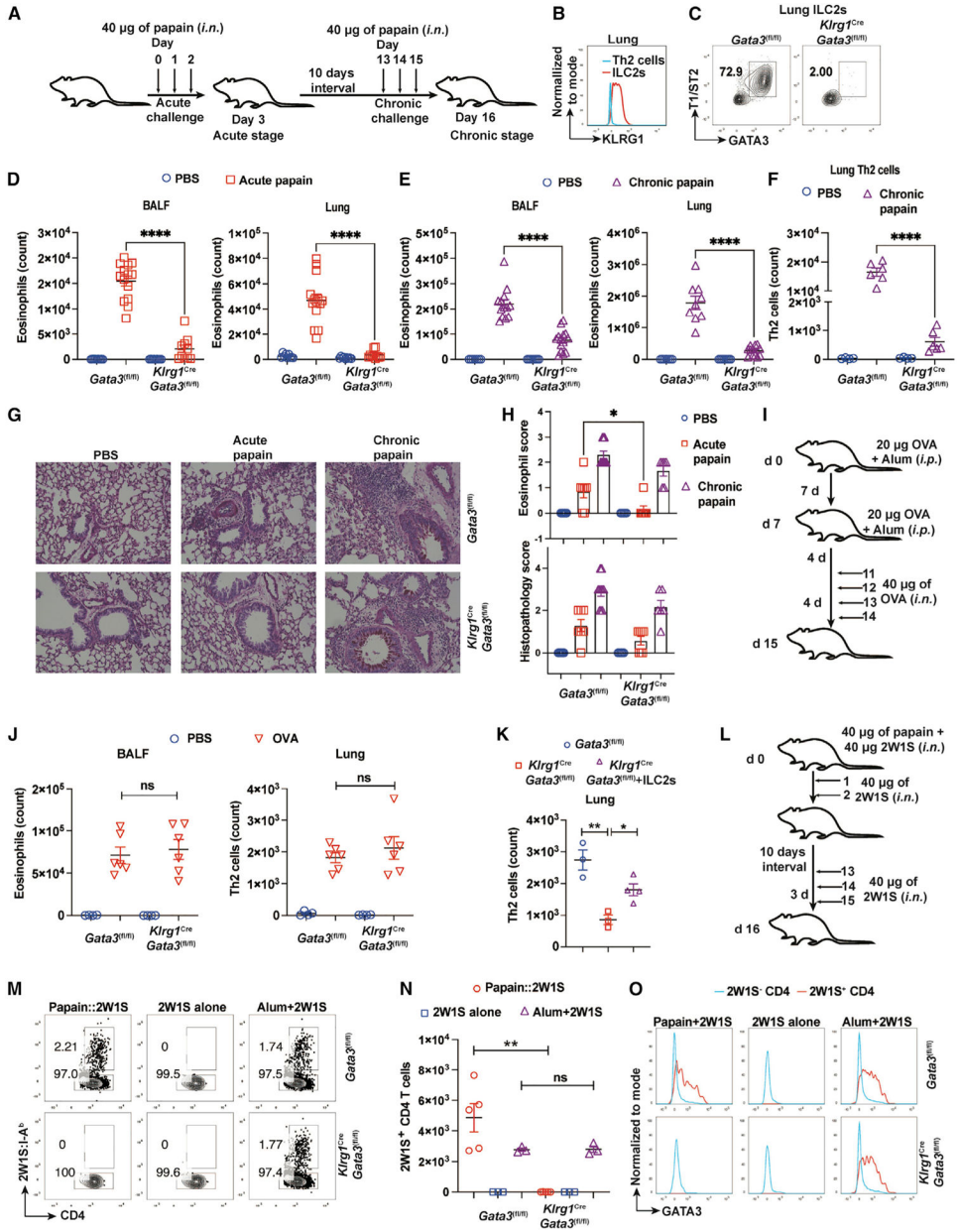

Figure 1. ILC2-dependent and -independent Th2 cell differentiation

(A) Experimental procedure for acute and chronic papain models.

(B) Flow cytometric histogram overlay showing the expression of KLRG1 on lung ILC2s ($CD45^+Lin^-IL\text{-}7R\alpha^+GATA3^+T1/ST2^+$) and Th2 cells ($CD45^+CD4^+Foxp3^-GATA3^+T1/ST2^+$) from WT mice chronically challenged with papain.

(C) ILC2s in the pulmonary tissue were compared between *Gata3*$^{fl/fl}$ and *Klrg1*^{Cre}*Gata3*$^{fl/fl}$ mice at the steady state by flow cytometry.

(D) *Gata3*$^{fl/fl}$ (WT) and *Klrg1*^{Cre}*Gata3*$^{fl/fl}$ (ILC2-deficient) mice were acutely challenged with papain. The total numbers of eosinophils infiltrated into BALF and lung were counted and plotted (mean ± SEM; n = 9–14; ****p < 0.0001, Student's t test).

(E) Mice were chronically challenged with papain followed by flow cytometric analysis of eosinophilic infiltration in BALF. The total numbers of eosinophils infiltrated into BALF and lung were counted and plotted (mean ± SEM; n = 7–14; ****p < 0.0001, Student's t test).
(F) Mice were chronically challenged with papain. The total numbers of Th2 cells in lung were counted and plotted (mean ± SEM; n = 4–6; ****p < 0.0001, Student's t test).
(G) Shown are the microscopic images of periodic acid-Schiff-stained lung tissue sections.
(H) Eosinophilic scores and total lung histopathology scores were plotted (mean ± SEM; n = 5–10; *p < 0.05, Student's t test).
(I) Experimental procedure for OVA-induced pulmonary allergy model.
(J) The total cell number of eosinophils and Th2 cells in mice treated in (I) were measured by flow cytometry, and the values were plotted (mean ± SEM; n = 4–6; ns, not significant, Student's t test).
(K) The ILC2-deficient mice were injected with ILC2s followed by chronic papain challenges. Th2 cells in the lung were analyzed by flow cytometry, and the total Th2 cell numbers were counted and plotted (mean ± SEM; n = 3–4; *p < 0.05, **p < 0.01, Student's t test).
(L) Experimental procedure for the generation of antigen-specific Th2 cells by papain:2W1S immunization.
(M) 2W1S-specific 2W1S:I-A^b tetramer$^+$ CD4$^+$ T cells were assessed by flow cytometry.
(N) The total numbers of 2W1S:I-A^b tetramer$^+$ CD4$^+$ T cells from (M) were counted and plotted (mean ± SEM; n = 3–5; ns, not significant, **p < 0.01, Student's t test).
(O) Flow cytometric analysis of GATA3 expression by 2W1S:I-A^b tetramer$^+$ CD4$^+$ T cells.
Results are representative of two (M–O) and three (B–H, J, and K) independent experiments. See also Figures S1–S3.

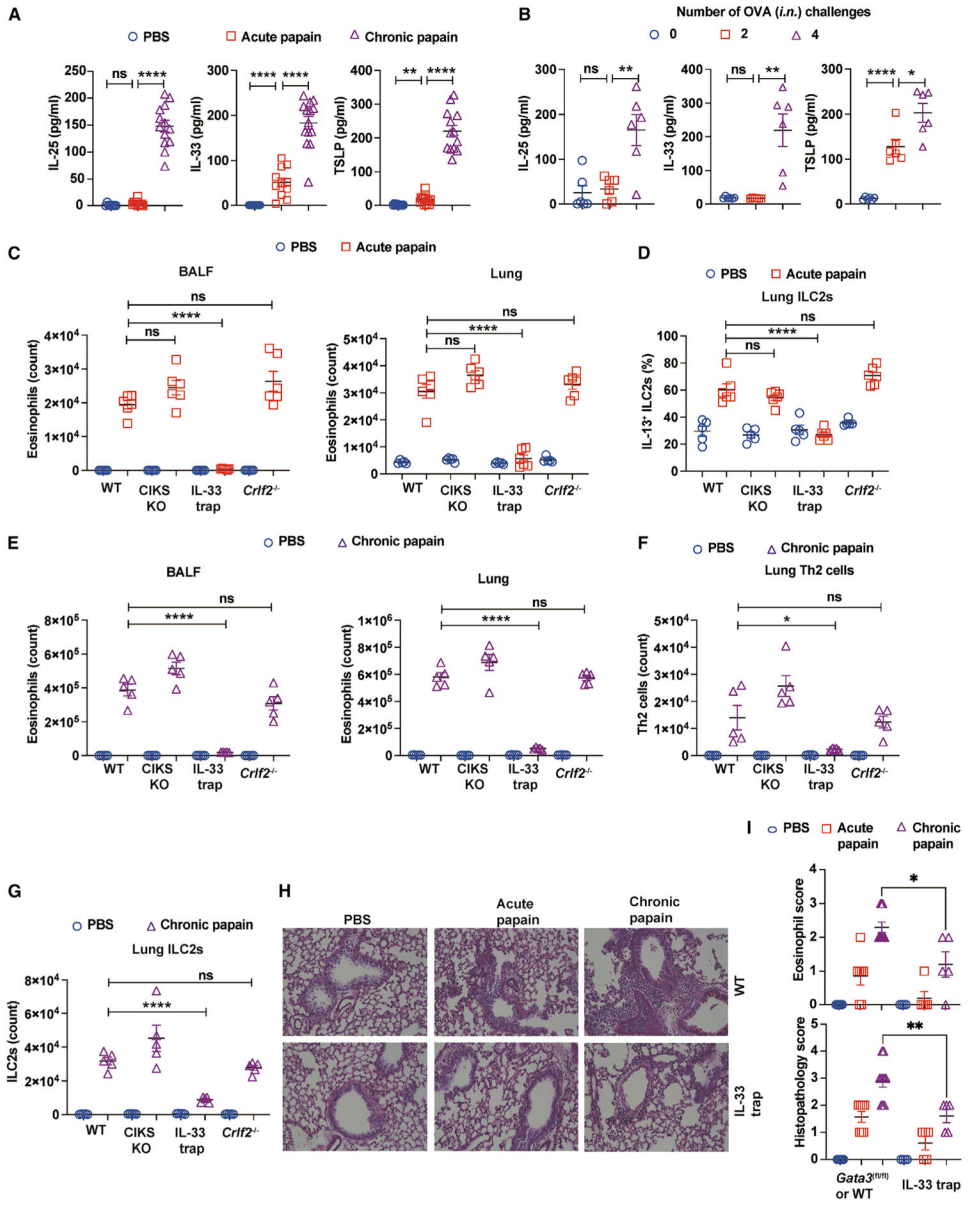

Figure 2. IL-33 is required for ILC2-mediated enhancement of Th2 cell response

(A) WT mice were challenged i.n. with PBS or papain and then sacrificed on day 3 (acute) or 16 (chronic). IL-25, IL-33, and TSLP were measured by ELISA (mean ± SEM; n = 8–14; ns, not significant, **p < 0.01, ****p < 0.0001, Student's t test).

(B) WT mice sensitized with OVA/alum or alum alone on days 0 and 7, followed by four doses of OVA i.n. challenges on days 11–14. These mice were sacrificed on days 11, 13, and 15. IL-25, IL-33, and TSLP were measured by ELISA (mean ± SEM; n = 8–11; ns, not significant, *p < 0.05, **p < 0.01, ****p < 0.0001, Student's t test).

(C and D) WT mice and mice deficient for CIKS, IL-33, and TSLPR are acutely challenged with PBS or papain, and mice were sacrificed on day 3.

(C) Eosinophils in BALF and lung were analyzed by flow cytometry. The total numbers were counted and plotted (mean ± SEM; n = 6; ****p < 0.0001, ns, not significant, Student's t test).
(D) Lung cells were stimulated with PMA/ionomycin, and then IL-13-producing ILC2s were analyzed by flow cytometry. Percentages of IL-13^+ ILC2s were calculated and plotted (mean ± SEM; n = 5–6; ****p < 0.0001, ns, not significant, Student's t test).
(E–G) Mice were chronically challenged with papain or PBS and sacrificed on day 16.
(E) Eosinophils in BALF and lung were analyzed by flow cytometry. The total numbers were counted and plotted (mean ± SEM; n = 5; ****p < 0.0001, ns, not significant, Student's t test).
(F) Th2 cells in the lung were analyzed by flow cytometry. The total numbers were counted and plotted (mean ± SEM; n = 5; *p < 0.05, ns, not significant, Student's t test).
(G) ILC2s in the lung were analyzed by flow cytometry. The total numbers were counted and plotted (mean ± SEM; n = 5; ****p < 0.0001, ns, not significant, Student's t test).
(H) Shown are the microscopic images of lung tissue sections stained with periodic acid-Schiff.
(I) Eosinophilic scores and total lung histopathology scores were plotted (mean ± SEM; n = 4–10; *p < 0.05, **p < 0.01, Student's t test).
Results are representative of at least two independent experiments. See also Figures S2 and S4.

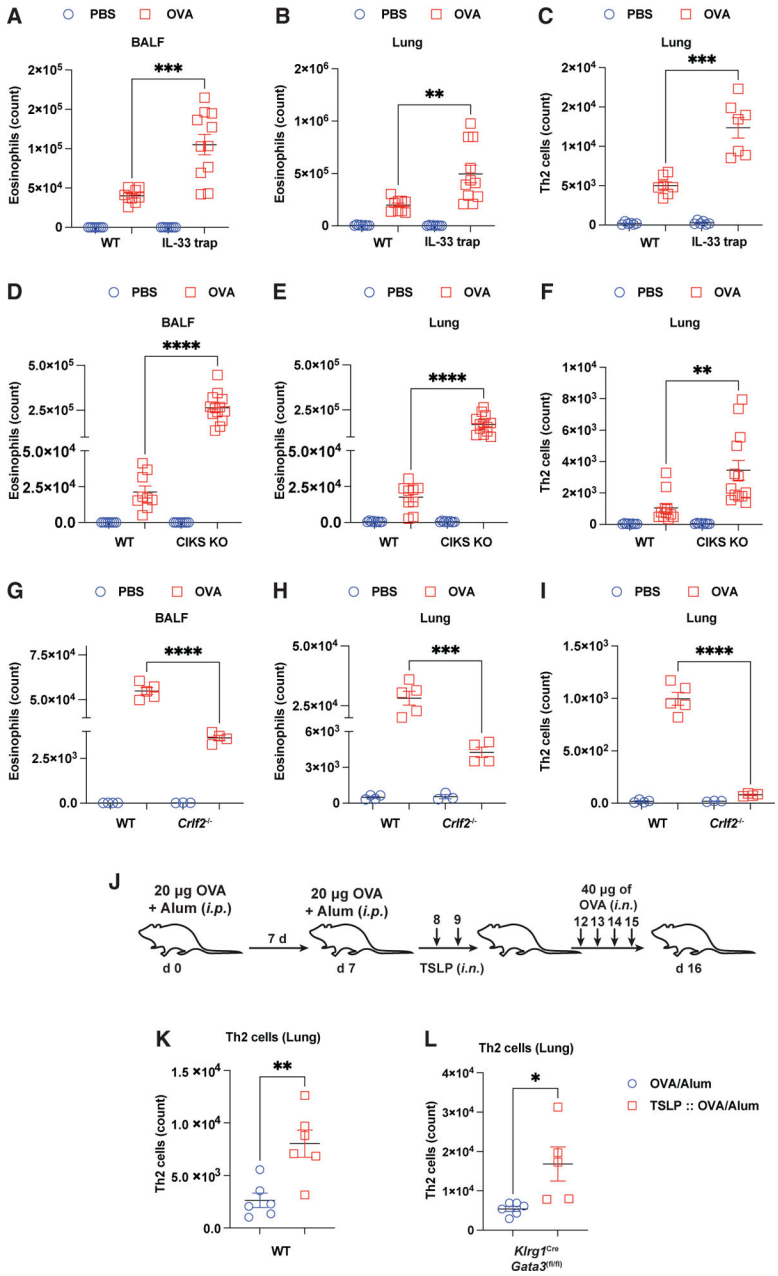

Figure 3. TSLP is important for ILC2-independent Th2 cell response

(A–I) OVA/alum-induced airway inflammation model was used as described in Figure 1I. The total cell numbers of eosinophil and Th2 cells were measured by flow cytometry, and the values were plotted (mean ± SEM; n = 4–12; **p < 0.01, ***p < 0.001, ****p < 0.0001, Student's t test).

(J) A modified experimental procedure for OVA-induced pulmonary allergy model for testing the effect of TSLP administration.

(K and L) The total cell numbers of Th2 cells in mice treated in (J) were measured by flow cytometry, and the values were plotted (mean ± SEM; n = 5–6; *p < 0.05, **p < 0.01, Student's t test).

Results are representative of two (G–I and K–L) to three (A–F) independent experiments. See also Figure S4.

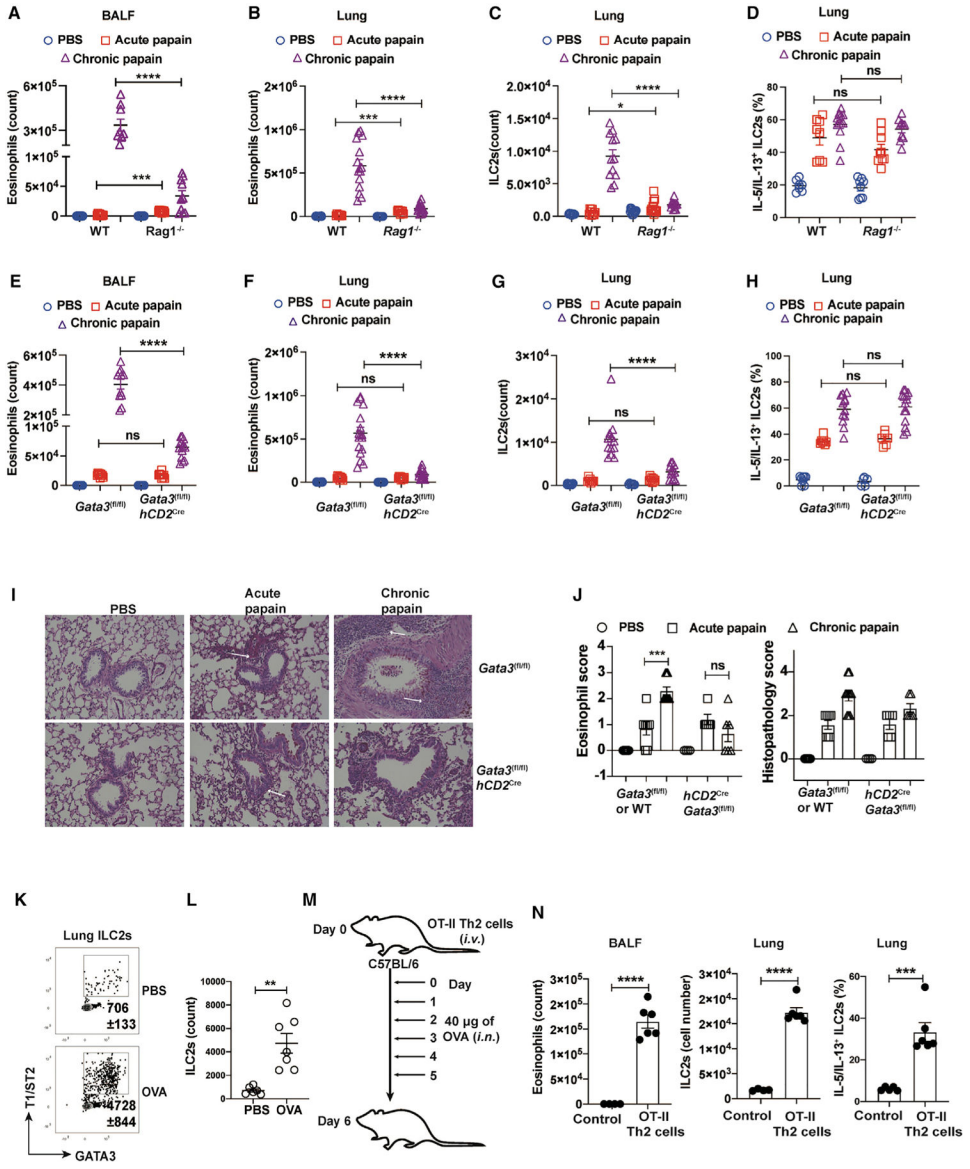

Figure 4. ILC2 expansion during chronic papain challenges requires Th2 cells

(A–D) WT and *Rag1*$^{-/-}$ mice were intranasally challenged with PBS or papain and then sacrificed on days 3 (acute) and 16 (chronic).

(A–C) Eosinophils in the BALF and lung and ILC2s in the lung were analyzed by flow cytometry. The total numbers of eosinophils in BALF (A) and lung (B) were counted and plotted (mean ± SEM; n = 7–12; ***p < 0.001, ****p < 0.0001, Student's t test). The total numbers of ILC2s (C) were counted and plotted (mean ± SEM; n = 9–15; *p < 0.05, ****p < 0.0001, Student's t test).

(D) Lung cells were stimulated with PMA/ionomycin, and then IL-5/IL-13-producing ILC2s were analyzed by flow cytometry. The percentage of ILC2s expressing IL-5/IL-13 were counted and plotted (mean ± SEM; n = 7–13; ns, not significant, Student's t test).

(E–H) *Gata3*$^{fl/fl}$ mice and h*CD2*^{Cre}*Gata3*$^{fl/fl}$ mice were challenged i.n. with PBS or papain and then sacrificed on days 3 (acute) and 16 (chronic).

(E and F) Eosinophils in BALF (E) and lung (F) were analyzed by flow cytometry. The total numbers were counted and plotted (mean ± SEM; n = 9–20; ns, not significant, ****p < 0.0001, Student's t test).

(G) ILC2s in the lung were analyzed by flow cytometry. The total numbers were counted and plotted (mean ± SEM; n = 7–16; *p < 0.05, ****p < 0.0001, Student's t test).

(H) Lung cells were stimulated with PMA/ionomycin, and then IL-5/IL-13-producing ILC2s were analyzed by flow cytometry. The percentage of ILC2s expressing IL-5/IL-13 were counted and plotted (mean ± SEM; n = 5–14; ns, not significant, Student's t test).

(I) Shown are the microscopic images of periodic acid-Schiff-stained lung tissue sections.

(J) Eosinophilic scores and total lung histopathology scores were plotted (mean ± SEM; n = 4–10; ns, not significant, ***p < 0.001, Student's t test).

(K) OVA-induced airway inflammation was performed with WT mice. ILC2s in the lung were analyzed by flow cytometry.

(L) The total numbers of ILC2s in (K) were counted and plotted (mean ± SEM; n = 6–7, **p < 0.01, Student's t test).

(M) Experimental procedure for pulmonary inflammation induced by *in-vitro*-differentiated OT-II-Th2 cell adoptive cell transfer.

(N) Eosinophils, ILC2s, and IL-5/IL-13-expressing ILC2s were analyzed by flow cytometry. The total numbers were then counted and plotted (mean ± SEM; n = 6; ***p < 0.001, ****p < 0.0001, Student's t test).

Results are representative of three independent experiments. See also Figure S5.

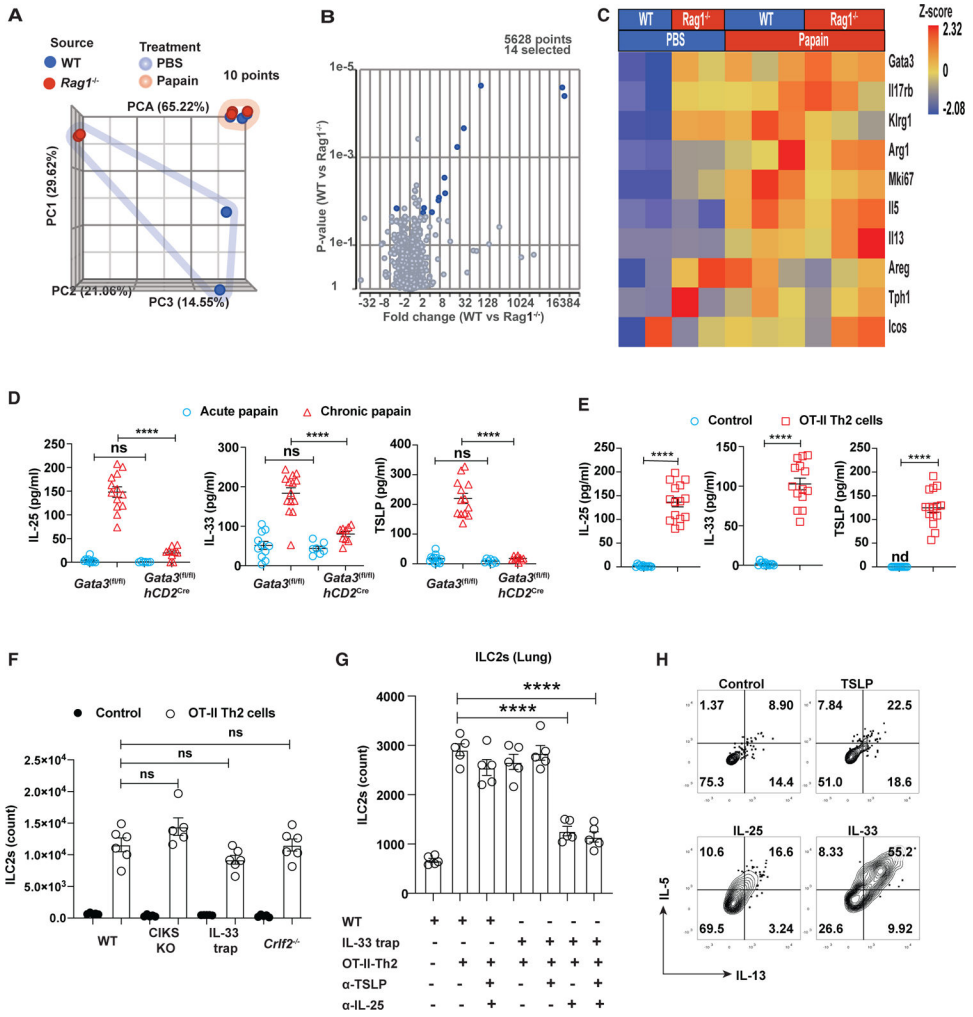

Figure 5. Type 2 alarmins induced by Th2 cells play a redundant role in ILC2 expansion

(A) PCA of RNA-seq data from sorted lung ILC2s after chronic papain challenges on day 16 (highlighted by pink) or with PBS as controls (highlighted by blue).

(B) Volcano plot showing few differentially expressed genes after papain challenges.

(C) Heatmap showing the expression of selected genes that are associated with type 2 immune responses. Heatmap color indicates the *Z* score.

(D) Type 2 alarmins in the BLAF of papain challenged mice on days 3 (acute) and 16 (chronic) were measured by ELSIA and plotted (mean ± SEM; n = 6–14; ****p < 0.0001, ns, not significant, Student's t test).

(E) Type 2 alarmins in the BLAF of WT mice that received OT-II Th2 cells and were challenged with OVA for 5 days were measured by ELISA (mean ± SEM; n = 12–15; ****p < 0.0001, Student's t test).

(F) The total cell numbers of ILC2s from mice that received OT-II Th2 cells and were challenged with OVA for 5 days were counted and plotted (mean ± SEM; n = 5–6; ns, not significant, Student's t test).

(G) The total cell numbers of ILC2s from mice that received OT-II Th2 cells and were challenged with OVA with or without indicated antibody treatment for 5 days were counted and plotted (mean ± SEM; n = 6; ****p < 0.0001, Student's t test).
(H) Flow cytometric analysis of IL-5 and IL-13 expression by pulmonary ILC2s from WT naive mice treated with various type 2 alarmins *in vitro*.
Results for RNA-seq experiment (A–C) are representative of one single experiment with biological duplicates (PBS) or triplicates (chronic papain). Results are representative of two (F and G) and three (D, E, and H) experiments.

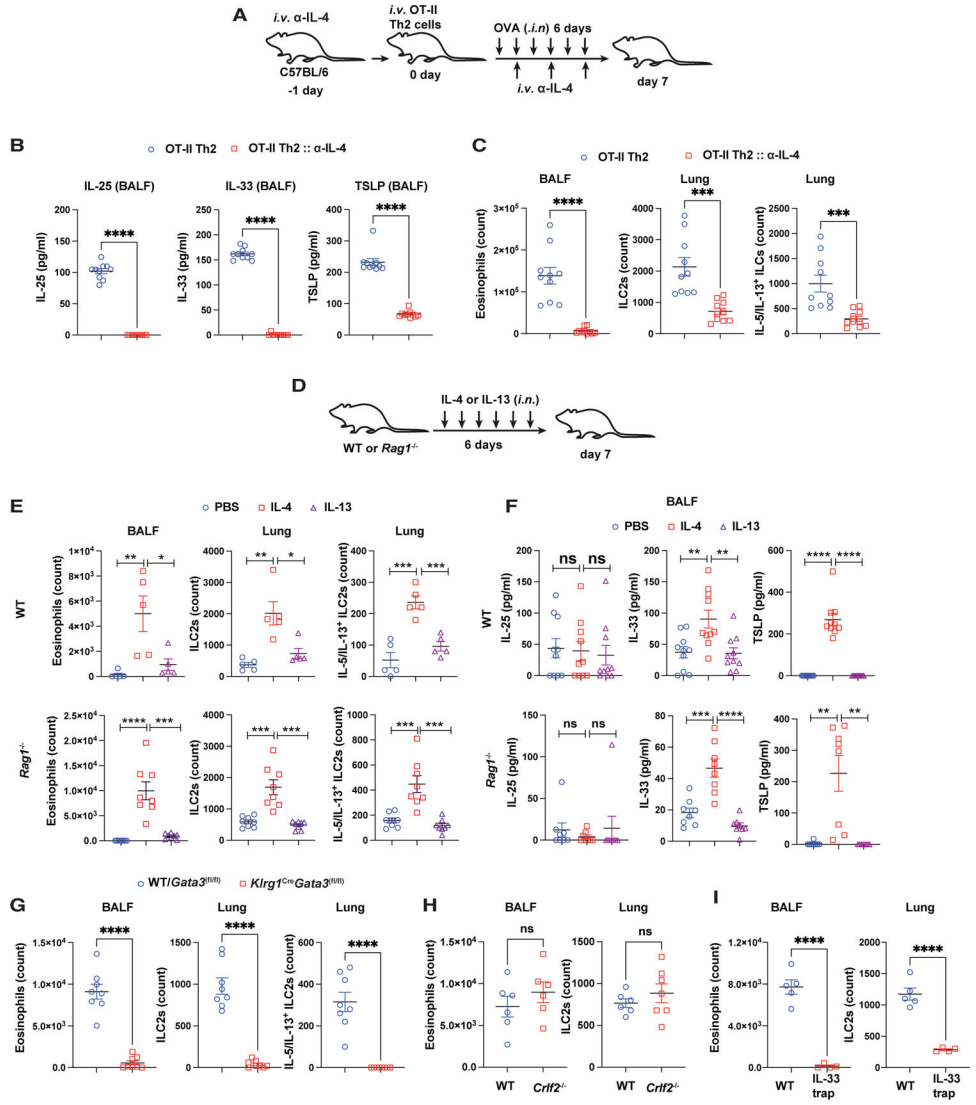

Figure 6. IL-4 is necessary and sufficient to induce ILC2 expansion and activation via regulating type 2 alarmins

(A) A modified experimental procedure for pulmonary inflammation induced by adoptive transfer of *in-vitro*-differentiated OT-II-Th2 cells when IL-4 was neutralized.

(B) The type 2 alarmin levels in the BALF were measured by ELISA, and the values were plotted (mean ± SEM; n = 10; ****p < 0.0001, Student's t test).

(C) The cell numbers of eosinophils and ILC2s measured by flow cytometry and plotted (mean ± SEM; n = 10; ***p < 0.001, ****p < 0.0001, Student's t test).

(D) Mouse model to study IL-4 and IL-13 effect on ILC2 response.

(E) The cell numbers of eosinophils and ILC2s for WT (top panel) and *Rag1*$^{-/-}$ (bottom panel) mice were measured by flow cytometry, and the values were plotted (mean ± SEM; n = 5; *p < 0.05, **p < 0.01, ***p < 0.001, ****p < 0.0001, Student's t test).

(F) The type 2 alarmin levels in the BALF were measured by ELISA. The values for WT (top panel) and *Rag1*$^{-/-}$ (bottom panel) mice were plotted (mean ± SEM; n = 5; ns, not significant, **p < 0.01, ***p < 0.001, ****p < 0.0001, Student's t test).

(G) The cell numbers of eosinophils and ILC2s in mice challenged i.n. with IL-4 were measured by flow cytometry, and the values were plotted (mean ± SEM; n = 8; ****p < 0.0001, Student's t test).
(H) The cell numbers of eosinophils and ILC2s in mice challenged i.n. with IL-4 were measured by flow cytometry, and the values were plotted (mean ± SEM; n = 6–7; ns, not significant, Student's t test).
(I) The cell numbers of eosinophils and ILC2s in mice challenged i.n. with IL-4 were measured by flow cytometry, and the values were plotted (mean ± SEM; n = 4–5; ****p < 0.0001, Student's t test).
Results are representative of two independent experiments. See also Figure S6.

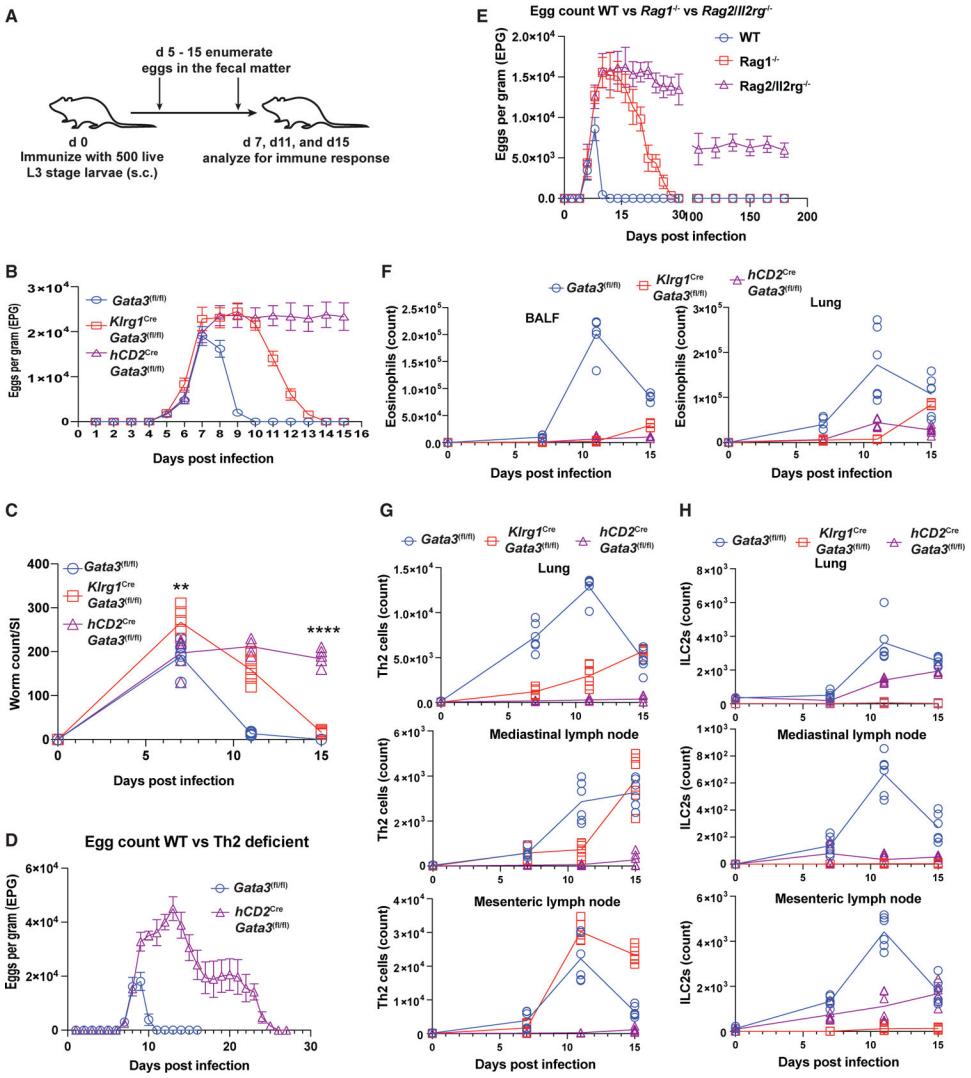

Figure 7. Temporally specific functions of ILC2s and Th2 cells and their crosstalk during *N. brasiliensis* infection

(A) Mice model of *N. brasiliensis* infection, egg enumeration, and worm counts.

(B–H) Mice were infected with L3 stage larvae. The fecal egg count was monitored throughout the study. Some mice were sacrificed on the indicated days to assess cellular phenotype in different organs. The number of adult worms was enumerated in the small intestine.

(B) The excreted eggs were enumerated and plotted as eggs per gram of fecal matter (EPG) (mean ± SEM; n = 4–10).

(C) Worm burden in the small intestine (worm count/SI) on different days post-infection (mean; n = 6, **p < 0.01, ****p < 0.0001, Student's t test).

(D) The excreted eggs were enumerated up to 30 days.

(E) The excreted eggs were enumerated up to 200 days.

(F) The total number of eosinophils in the BALF and lung was measured by flow cytometry and plotted (mean; n = 3–6).

(G) The total number of Th2 cells in different organs was measured by flow cytometry and plotted (mean; n = 3–6).
(H) The total number of ILC2s in different organs was measured by flow cytometry and plotted (mean; n = 3–6). Results are representative of two (D and E) and three (B, C, and F–H) independent experiments. See also Figure S7.

KEY RESOURCES TABLE

REAGENT or RESOURCE	SOURCE	IDENTIFIER
Antibodies		
Purified anti-mouse CD16/32 antibody (Clone# 93)	BioLegend	Cat#101302; RRID: AB_312801
CD45 Antibody (Clone# 30–F11), Brilliant Violet 650™	BioLegend	Cat#103151; RRID: AB_2565884
CD45 Antibody (Clone# 30–F11), Brilliant Violet 785™	BioLegend	Cat#103149; RRID: AB_2564590
Siglec-F Antibody (Clone# E50–2440), Alexa Fluor® 647	BD Biosciences	Cat#562680; RRID: AB_2687570
IL-5 Antibody (Clone# TRFK5), APC	BD Biosciences	Cat#554396; RRID: AB_398548
IL-4 Monoclonal Antibody (Clone# 11B11), PE	eBioscience	Cat#12–7041–82; RRID: AB_466156
IL-13 Monoclonal Antibody (Clone# eBio13A), PE-Cyanine7	eBioscience	Cat#25–7133–82; RRID: AB_2573530
IL-13 Monoclonal Antibody (Clone# eBio13A), PerCP-eFluor 710	eBioscience	Cat#46–7133–82; RRID: AB_11218496
IFN-γ Antibody (Clone# XMG1.2), Brilliant Violet 605™	BioLegend	Cat#505840; RRID: AB_2734493
CD4 Antibody (Clone# RM4–5), V500	BD Biosciences	Cat#560782; RRID: AB_1937327
CD4 Antibody (Clone# GK1.5), Brilliant Violet 605™	eBioscience	Cat#100451; RRID: AB_2564591
CD4 Antibody (Clone# GK1.5), Alexa Fluor® 700	BioLegend	Cat# 100430; RRID: AB_493699
CD45RB Antibody (Clone# C363.16A), APC	eBioscience	Cat# 17–0455–81; RRID: AB_2565431
CD25 Monoclonal Antibody (PC61.5), PE-Cyanine7	eBioscience	Cat# 25–0251–82; RRID: AB_469608
CD11b Antibody (Clone# RM4–5), Brilliant Violet 605™	BioLegend	Cat#101257; RRID: AB_2565431
CD11b Monoclonal Antibody (Clone# M1/70), eFluor™ 450	eBioscience	Cat#48–0112–82; RRID: AB_1582236
CD103 Antibody (Clone# 2E7), Brilliant Violet 785™	BioLegend	Cat#121439; RRID: AB_2800588
Purified anti mouse IL-25 antibody (Clone# 35B)	BioLegend	Cat#514401; RRID: AB_2043954
Purified anti mouse TSLP antibody (Clone# 28F12)	BioLegend	Cat#515202; RRID: AB_2561323
CD40 Antibody (Clone# 3/23), PE/Cyanine5	BioLegend	Cat#124618; RRID: AB_2075922
CD40 Antibody (Clone# 1C10), PE	eBioscience	Cat#12–0401–82; RRID: AB_465649
KLRG1 (MAFA) Antibody (Clone# 2F1/KLRG1), Brilliant Violet 711™	BioLegend	Cat#138427; RRID: AB_2629721
CD45R/B220 Antibody (Clone# RA3–6B2), PerCP	BioLegend	Cat#103234; RRID: AB_893353
CD45R (B220) Monoclonal Antibody (Clone# RA3–6B2), eFluor™ 450	eBioscience	Cat#48–0452–82; RRID: AB_1548761
CD49a Monoclonal Antibody (Clone# HMα1), PE	BioLegend	Cat#142604; RRID: AB_10945158
CD49b Monoclonal Antibody (Clone# HMα2), PE/Cyanine7	BioLegend	Cat#103518; RRID: AB_2566103
NK-1.1 Monoclonal Antibody (Clone# PK136), Brilliant Violet 605	BioLegend	Cat#108753; RRID: AB_2686977

REAGENT or RESOURCE	SOURCE	IDENTIFIER
CD335 (NKp46) Monoclonal Antibody (Clone# 29A1.4), Brilliant Violet 711	BioLegend	Cat#137621; RRID: AB_2563289
T1/ST2 (IL-33 R) Monoclonal Antibody (Clone# DJ8), PE	MD Bioproducts	Cat#101001PE
T1/ST2 (IL-33 R) Monoclonal Antibody (Clone# DJ8), FITC	MD Bioproducts	Cat#101001F
CD127 Monoclonal Antibody (Clone# A7R34), FITC	eBioscience	Cat#11–1271–82; RRID: AB_465195
CD127 Monoclonal Antibody (Clone# A7R34), Alexa Fluor 700	eBioscience	Cat#56–1271–82; RRID: AB_657611
CD127 Monoclonal Antibody (Clone# eBioRDR5), PE-Cyanine7	eBioscience	Cat#25–1278–42; RRID: AB_1659672
CD11c Monoclonal Antibody (Clone #N418), eFluor 450	eBioscience	Cat#48–0114–82; RRID: AB_1548654
CD3e Monoclonal Antibody (Clone# 145–2C11), eFluor™ 450	eBioscience	Cat#48–0031–82; RRID: AB_10735092
TCR gamma/delta Monoclonal Antibody (Clone# eBioGL3), eFluor™ 450	eBioscience	Cat#48–5711–82; RRID: AB_2574071
CD5 Monoclonal Antibody (Clone 53–7.3), eFluor™ 450	eBioscience	Cat#48–0051–80; RRID: AB_1603252
Ly-6G/Ly-6C Monoclonal Antibody (Clone# RB6–8C5), eFluor™ 450	eBioscience	Cat#48–5931–82; RRID: AB_1548788
Ly-6G/Ly-6C Monoclonal Antibody (Clone# RB6–8C5), APC-eFluor 780	eBioscience	Cat#47–5931–82; RRID: AB_1518804
FcεRIα Monoclonal Antibody (Clone# MAR-1), Pacific Blue	BioLegend	Cat#134314; RRID: AB_10613298
FOXP3 Monoclonal Antibody (Clone# FJK-16s), eFluor™ 450	eBioscience	Cat#48–5773–82; RRID: AB_1518812
FOXP3 Monoclonal Antibody (Clone# FJK-16s), PE	eBioscience	Cat#12–5773–82; RRID: AB_465936
FOXP3 Monoclonal Antibody (Clone# MF23), R718	BD Biosciences	Cat#567095
Gata3 Monoclonal Antibody (Clone# TWAJ), Alexa Fluor™ 488	eBioscience	Cat#53–9966–42; RRID: AB_2574493
Gata3 Monoclonal Antibody (Clone# TWAJ), eFluor™ 660	eBioscience	Cat#50–9966–42; RRID: AB_10596663
Gata3 Monoclonal Antibody (Clone# TWAJ), PE-eFluor™ 610	eBioscience	Cat#61–9966–42; RRID: AB_2574686
ROR gamma (t) Monoclonal Antibody (Clone# B2D), PE-eFluor 610	eBioscience	Cat#61–6981–82; RRID: AB_2574650
ROR gamma (t) Monoclonal Antibody (Clone# Q31–378), BV650	BD Biosciences	Cat#564722; RRID: AB_2738915
T-bet Monoclonal Antibody (Clone# eBio4B10 (4B10)), PE-Cyanine7	eBioscience	Cat#25–5825–82; RRID: AB_11042699
Anti-CD3e (Clone 2C11)	Harlan	Lot#A2022931
Anti-CD28 (Clone 37.51)	Harlan	Lot#A2022929
Anti-IFN-γ (Clone XMG1.2)	Harlan	Lot#A2022930
Anti-IL-4 (Clone 11B.11)	Harlan	Lot#A2022930
Anti-CD16/CD32 (Clone 2.4G2)	Harlan	Lot#A2083015
Dynabeads™ Mouse T-Activator CD3/CD28 for T cell Expansion and Activation	ThermoFisher	Cat#11452D
Chemicals, peptides, and recombinant proteins		
Peptide: 2W1S (EAWGALANWAVDSA)	GenScript	Cat#SC1208
Tetramer: 2W1S: IAb (I-A(b): EAWGALANWAVDSA-PE)	NIH Tetramer Facility	N/A

REAGENT or RESOURCE	SOURCE	IDENTIFIER
Albumin from chicken egg white	Sigma-Aldrich	Cat#A5503
Imject™ Alum Adjuvant	ThermoFisher	Cat#77161
Papain, Carica papaya	Sigma-Aldrich	Cat#5125
UltraComp eBeads™ Plus Compensation Beads	eBioscience	Cat#01–3333–42
Recombinant Mouse IL-1 β	R&D Systems	Cat#401-ML
Recombinant Mouse IL-2 protein	R&D Systems	Cat#402-ML
Recombinant Mouse IL-4 Protein	R&D Systems	Cat#404-ML
Recombinant Mouse IL-6 Protein	PeproTech	Cat#216–16
Recombinant Mouse IL-7 Protein	R&D Systems	Cat#407–ML–005
Recombinant Mouse IL-12 Protein	PeproTech	Cat#210–12
Recombinant Mouse IL-13 Protein	R&D Systems	Cat#413–ML–005
Recombinant Mouse IL-25 (IL-17E)	BioLegend	Cat#587302
Recombinant Mouse IL-33 Protein	R&D Systems	Cat#3626–ML
Recombinant Mouse TSLP Protein	R&D Systems	Cat#555–TS–010/CF
Recombinant Mouse TGF-P1 Protein	R&D Systems	Cat#7666–MB
SYBR™ Safe DNA Gel Stain	ThermoFisher	Cat#S33102
Platinum™ Hot Start PCR Master Mix (2X)	ThermoFisher	Cat#13000012
DNA Gel Loading Dye	ThermoFisher	Cat#R0611
100 bp DNA Ladder	ThermoFisher	Cat#15628019
HBSS, calcium, magnesium	ThermoFisher	Cat#24020117
ACK Lysing Buffer	ThermoFisher	Cat#A1049201
Collagenase, Type IV, powder	ThermoFisher	Cat#17104019
DNase I recombinant grade I, from bovine pancreas, expressed in Pichia pastoris	Roche	Cat#4536282001
PBS, pH 7.4	ThermoFisher	Cat#10010031
Albumin, Bovine Fraction V	MP	Cat#160069
RPMI 1640 Medium	ThermoFisher	Cat#21870–076
Fetal Bovine Serum	R&D Systems	Cat#S12450
Penicillin-Streptomycin	ThermoFisher	Cat#15140122
L-Glutamine (200 mM)	ThermoFisher	Cat#25030081
MEM Non-Essential Amino Acids Solution (100X)	ThermoFisher	Cat#11140050
Sodium Pyruvate	ThermoFisher	Cat#11360

REAGENT or RESOURCE	SOURCE	IDENTIFIER
2-Mercaptoethanol	ThermoFisher	Cat#21985023
E-Gel™ SizeSelect™ II Agarose Gels, 2%	ThermoFisher	Cat#G661012
Nystatin	Sigma-Aldrich	Cat#N6261–500KU
Activated charcoal	Sigma-Aldrich	Cat#C2764–500G
Phorbol 12-myristate 13-acetate	Sigma-Aldrich	Cat#P8139–5MG
Ionomycin	Sigma-Aldrich	Cat#407952–5MG
Brefeldin A Solution	BioLegend	Cat#420601
Qiazol lysis reagent	QIAGEN	Cat#79306
DMSO	Sigma-Aldrich	Cat#D2650
1000 ML PREFILLED FORMALIN CONTAINER	Azer Scientific	Cat#PFNBF-1000
eBioscience™ Foxp3/Transcription Factor Staining Buffer Set	eBioscience	Cat#00–5523–00
Fixable Viability Dye eFluor™ 780	eBioscience	Cat#65–0865–14
Critical commercial assays		
Mouse IL-17E Duoset ELISA	R&D Systems	Cat#DY1399
Mouse IL-33 DuoSet ELISA	R&D Systems	Cat#DY3626–05
Mouse TSLP Quantikine ELISA kit	R&D Systems	Cat#MTLP00
Qubit™ RNA High Sensitivity (HS), Assay Kit	ThermoFisher	Cat#Q10210
Qubit™ dsDNA Broad Rang (BR) Assay Kit	ThermoFisher	Cat#Q32850
RNeasy Micro Kit (50)	QIAGEN	Cat#74004
MinElute Gel Extraction Kit (50)	QIAGEN	Cat#28604
MinElute Reaction Cleanup Kit	QIAGEN	Cat#28206
RNase-Free DNase Set	QIAGEN	Cat#79256
Ovation® RNA-Seq System V2	TECAN	Cat#7102–32
KAPA LTP Library Preparation Kit	Roche	Cat#KK8232
Naive CD4 T cell isolation Kit mouse	Miltenyi Biotec	Cat#130–104–453
EasySep™ Mouse ILC2 Enrichment Kit	STEMCELL	Cat#19842
Deposited data		
RNA-Seq Raw and analyzed data	This paper	GEO: GSE166779
Experimental models: Organisms/strains		
Mouse: *KIrg1*^{Cre}; strain background: C57BL/6	Dr. Richard Flavell of Yale University	Herndler-Brandstetter et al.[27]

REAGENT or RESOURCE	SOURCE	IDENTIFIER
Mouse: *Gata3*$^{fl/fl}$; strain background: C57BL/6	NIAID-Taconic repository	Zhu et al.[14] (Line 355)
Mouse: *hCD2*^{Cre}; strain background: C57BL/6	Dr. Paul Love of NICHD, NIH	Vacchio et al.[51] (also available as JAX line: 027406)
Mouse: *Crlf2*$^{-/-}$;strain background: C57BL/6	Dr. Warren J. Leonard of NHLBI, NIH	Al-Shami et al.[36]
Mouse: IL-33 KO (IL-33 trap); strain background: C57BL/6	Late Dr. William E. Paul of NIAID, NIH	Pichery et al.[35]
Mouse: CIKS KO; strain background: C57BL/6	NIAID-Taconic repository	Line: 290
Mouse: *Rag1*$^{-/-}$; B6.SJL-[KO]RAG1	NIAID-Taconic repository	Line: 165
Mouse: *Rag2*$^{-/-}$*Il2rg*$^{-/-}$; C57BL/10SgSnAi-[KO]RAG2-[KO]gamma c	NIAID-Taconic repository	Line: 111
Mouse: OT-II; B6.SJL-Ptprc^{a} Rag1^{tm1} Tg(TcraTcrb)425Cbn	NIAID-Taconic repository	Line: 361
Mouse: C57BL/6 (B6NTac)	Taconic	C57BL/6NTac
Mouse: *Il4*$^{-/-}$; strain background: C57BL/6	NIAID-Taconic repository	Line: 46
Mouse: *Il4/Il13*$^{-/-}$; strain background: C57BL/6	NIAID-Taconic repository	Line: 242
Oligonucleotides		
please see Table S1 for Oligo sequences	IDT	N/A
Software and algorithms		
FlowJo V10	FlowJo LLC	https://www.flowjo.com
Partek Flow	Partek	https://www.partek.com
GraphPad Prism	GraphPad	https://www.graphpad.com